

This is an Open Access document downloaded from ORCA, Cardiff University's institutional repository: <https://orca.cardiff.ac.uk/id/eprint/138743/>

This is the author's version of a work that was submitted to / accepted for publication.

Citation for final published version:

Deng, Lanfeng, Zhang, Yahui and Kennedy, David 2021. Dynamics of 3D sliding beams undergoing large overall motions. *Communications in Nonlinear Science and Numerical Simulation* 98 , 105778. 10.1016/j.cnsns.2021.105778

Publishers page: <http://dx.doi.org/10.1016/j.cnsns.2021.105778>

Please note:

Changes made as a result of publishing processes such as copy-editing, formatting and page numbers may not be reflected in this version. For the definitive version of this publication, please refer to the published source. You are advised to consult the publisher's version if you wish to cite this paper.

This version is being made available in accordance with publisher policies. See <http://orca.cf.ac.uk/policies.html> for usage policies. Copyright and moral rights for publications made available in ORCA are retained by the copyright holders.



# **Dynamics of 3D sliding beams undergoing large overall motions**

Lanfeng Deng<sup>a</sup>, Yahui Zhang<sup>a\*</sup>, David Kennedy<sup>b</sup>

*<sup>a</sup> State Key Laboratory of Structural Analysis for Industrial Equipment, Department of Engineering Mechanics, International Center for Computational Mechanics, Dalian University of Technology, Dalian 116023, PR China;*

*<sup>b</sup> School of Engineering, Cardiff University, Cardiff CF24 3AA, Wales, UK*

Corresponding author:

Dr. Y. H. Zhang

State Key Laboratory of Structural Analysis for Industrial Equipment, Department of Engineering Mechanics, Dalian University of Technology, Dalian 116023, PR China

Email: zhangyh@dlut.edu.cn

Tel: +86 411 84706337

Fax: +86 411 84708393

## Abstract

This paper presents the 3D dynamic formulations for a flexible beam sliding through a revolute-prismatic joint. Considering the geometric nonlinearity, the configuration space of the 3D flexible beam is a nonlinear differentiable manifold ( $\mathbb{R}^3 \times SO(3)$ ). Moreover, the beam manipulated by the revolute-prismatic joint can undergo large overall motion and slide through the joint. Because of the difficulty mentioned above, most studies on these problems focus on 2D cases or are tackled under a small deformation assumption. In this paper, the rotation matrices are parameterized using rotational vectors to describe accurately the spatial configuration of flexible beams. For convenience, to describe the finite deformation of the beams, the material frame is fixed on the revolute-prismatic joint but will change over time. The corotational method is introduced to take the geometric nonlinearity (small strain and large rotation) of the beam into account. In the corotational frame, the strain energy and kinetic energy of the elements are derived with the same shape functions, which are used to describe the local displacements, to maintain the element-independent framework. Then a ‘standard element’ can be embedded within this framework. In order to consider the shear deformation, the flexible beam is discretized using a fixed number of variable-domain interdependent interpolation elements. Rotary inertia is also considered in this paper. The nonlinear equations of motion are derived by using the extended Hamilton’s principle and solved by using the Hilber-Hughes-Taylor method and the Newton-Raphson iteration method. Four examples

are presented to demonstrate the validity, accuracy and versatility of the present dynamic formulation.

Keywords: co-rotational method; flexible robot manipulator; variable-domain beam elements; nonlinear dynamic analysis; rotating-prismatic joint

## 1. Introduction

Robot manipulator arms are widely used in engineering. Generally speaking, their weight should be as light as possible to reduce the cost and the energy consumption. But less material means the arms are more flexible. Thus the dynamic analysis of the flexible arms will be difficult, because their vibration involves not only the rigid motion but also the large elastic deformation. If the arms are manipulated by a revolute joint or a prismatic joint, the dynamic analysis will also be more difficult.

Many researchers used the sliding beam model to study the dynamics of robot manipulator arms with prismatic joints. The nonlinear equations of motion of sliding beams were firstly given by Tabarrok et al. [1] through Newton's Second Law. To obtain the approximate solution, they introduced small deformation and inextensibility assumptions. The equations of motion were also used to investigate band saws, spacecraft antenna and copy machines [2-4]. To take the geometric nonlinearity into account, Behdinan et al. [5, 6] derived the nonlinear equations of motion through an extension of

Hamilton's principle [7]. Then they used the Galerkin's method to solve the equations. Gürgöze and Yüksel [8] further investigated the effects of rotary inertia, end-mass and axial force in association with axial foreshortening. Stylianou and Tabarrok [9] used a fixed number of variable-domain beam elements to discretize the linear system of a sliding beam. Behdinan and Tabarrok [10] used the updated Lagrangian method [11] and co-rotational method [12] to derive the dynamic formulations for sliding beams respectively and discussed the effects of geometric nonlinearity on the dynamic response of the beam [13]. However, their formulations cannot maintain the consistency of the element because the elastic force vector and the inertia force vector are derived using different shape functions. In addition, the shape functions are used to describe the global displacement field rather than the local displacement field for the derivation of the inertia force vector. To take into account the deformation of the inside part of a sliding beam, Humer [14] presented dynamic formulations of a sliding beam with non-material boundary conditions where the position of the prismatic joint relative to the material points of the beam is unknown. Steinbrecher et al. [15] further used commercial software, ABAQUS, to study the sliding beam problem. Dilpare [16], Banerjee and Kane [17] used multibody dynamics to study the nonlinear motion of the sliding beam.

Some researchers studied the dynamics of robot manipulator arms with revolute joints. In studying the dynamic problem, a convenient method is to introduce a floating frame [18, 19] which allows the potential energy of the beam to be expressed in a simple

form with the assumption of small strains. By contrast, the expression of the kinetic energy of the system will be cumbersome. To overcome this difficulty, Simo and Vu-Quoc [20-25] derived the equations of motion of the beam in the inertial frame and took the geometric nonlinearity into account. McRobie and Lasenby [26] further presented a new formulation of Simo-Vu Quoc rods based on geometric algebra [27]. This formulation is easier to learn and manipulate. Damaren and Sharf [28] studied how nonlinear terms in the equations of motion of the beam influence the responses. To capture the motion-induced stiffness terms which are associated with the high-speed rotation of the beam, Liu and Hong [29] used non-Cartesian deformation variables to derive the equations of motion of the flexible beam. Similarly, Kane et al. [30] and Yoo et al. [31] studied the 3D dynamic problem of a beam attached to a moving rigid base under a small deformation assumption. Wu et al. [32] further took into account the geometric nonlinearity of the flexible beam.

A beam manipulated by a revolute-prismatic joint can either slide through the joint or undergo large overall motion. Yuh and Young [33] derived the equations of motion of the dynamic problem through Newton's Second Law. They used the assumed mode method to obtain approximate solutions and validated the model by experiments. In order to consider geometric nonlinearity and shear deformation of the flexible beam, Vu-Quoc and Li [34] studied the dynamic problems based on geometrically exact theory [22]. Al-Bedoor and Khulief [35] used a fixed number of constant-domain elements to discretize

the sliding beam. To deal with the time-dependent boundary condition at the channel orifice, they introduced a transition element with variable stiffness. Kalyoncu [36] proposed a mathematical model of a flexible robot manipulator with special boundary conditions such that the tip end of the manipulator traces a multi-straight-line path. Rotary inertia, axial shortening and gravitation were also considered in the model.

The aforementioned studies are all aimed at 2D problems, while most mechanical devices in engineering practice move in 3D space. The dynamic analysis of the 3D problems becomes more difficult for that the configuration space of the 3D flexible beam is a nonlinear differentiable manifold ( $\mathbb{R}^3 \times \text{SO}(3)$ ). Recently, Korayem et al. [37, 38] derived the equations of motion of N-flexible link manipulators. But they did not take account of the large deformations of the flexible beam.

In this paper, the model proposed by Vu-Quoc and Li [33] is extended to the 3D case. A flexible beam manipulated by a revolute-prismatic joint will not only undergo large overall motion but also slide through the joint. To investigate the geometric nonlinear dynamic problem of this kind of structures, the corotational method [39-41], which has high accuracy and efficiency [41], is used. The key idea of the corotational method is to decompose the motion of the element into rigid body motion and pure deformation. By introducing a rotational frame, the rigid body motions generated by not only the deformation of the beam but also the revolute-prismatic joint can be removed conveniently. Then, the pure deformation of the element can be easily measured in the

rotational frame (the local system). Different assumptions can be made to describe the local deformation of the element. In addition, the strain energy and kinetic energy of the elements are derived with the same shape functions to ensure the consistency of the element. The above element-independent framework is consistent with the idea of Nour-Omid and Rankin's [39, 40] corotational method. Then, a 'standard beam element' can be embedded within the framework. To consider the shear deformation and rotary inertia, the interdependent interpolation element (IIE) [42] is embedded within the framework. Because the material configuration of the beam will change with time, variable-domain IIEs are used to discretize the system in space. The Hilber-Hughes-Taylor method (HHT) [43, 44] is used to discretize the system in time to maintain the numerical stability.

## 2. 3D beam kinematics

As shown in Fig. 1, a flexible beam manipulated by a revolute-prismatic joint can slide through the joint and undergo large overall motion. The deformation of the beam can be decomposed into a rigid motion manipulated by the joint (Fig. 1) and a superposed finite deformation (Fig. 2). To describe the finite deformation conveniently, the sliding undeformed beam (Fig. 1) is chosen as the material configuration. Interest is confined to the deformation of the part outside the joint channel of the material beam. The time-varying material configuration can be expressed as

$$\mathcal{B}_m = \left\{ (X_1, X_2, X_3) \in \mathbb{R}^3 \mid X_1 \in [0, L(t)], X_2 \in \left[-\frac{h}{2}, \frac{h}{2}\right], X_3 \in \left[-\frac{b}{2}, \frac{b}{2}\right] \right\} \quad (1)$$



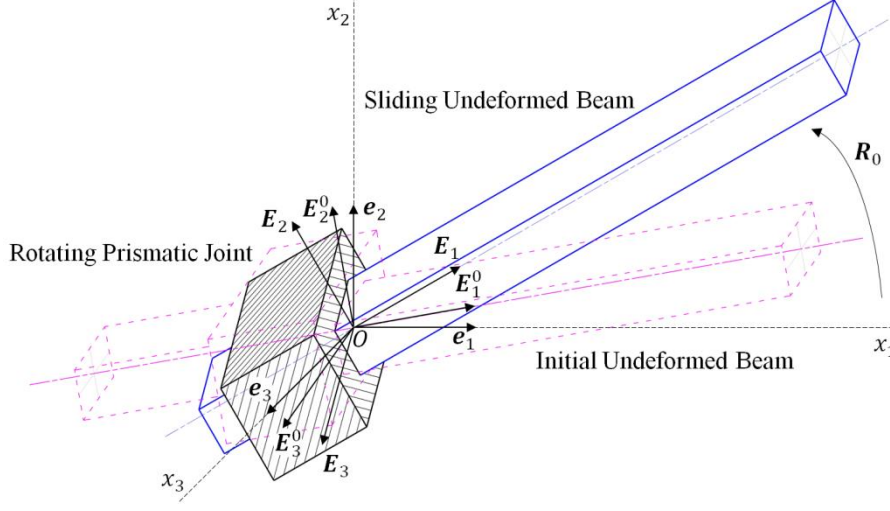


**Fig. 1** Description of the rigid motion of the beam

where  $L(t)$ ,  $h$  and  $b$  are the length, height and width of the material beam outside the joint channel, respectively. The material frame  $\{\mathbf{E}_1, \mathbf{E}_2, \mathbf{E}_3\}$  is fixed on the revolute-prismatic joint. The origin  $O$  of the material coordinate system is located at the center of the channel orifice. An inertial coordinate system  $(x_1, x_2, x_3) \in \mathbb{R}^3$  is set up for the spatial configuration  $\mathcal{B}_s$  with basis vectors  $\{\mathbf{e}_1, \mathbf{e}_2, \mathbf{e}_3\}$ . The spatial and material coordinate systems have the same origin. The relationship between the material and spatial basis vectors can be denoted by

$$\mathbf{E}_i = \mathbf{R}_0(t)\mathbf{e}_i, \quad i = 1, 2, 3 \quad (2)$$

where  $\mathbf{R}_0(t) = [\mathbf{r}_1^0, \mathbf{r}_2^0, \mathbf{r}_3^0] \in \text{SO}(3)$  is a prescribed orthogonal matrix and  $\text{SO}(3)$  is the noncommutative Lie group [45].

A plane cross-section assumption is introduced. At an arbitrary material point  $\mathbf{P} =$

$(X, 0, 0) \in \mathcal{B}_m$  of the beam centroidal line, an orthonormal frame  $\{\mathbf{t}_1(X), \mathbf{t}_2(X), \mathbf{t}_3(X)\}$  may be defined which can describe the finite rotations of the cross-section corresponding to the point.  $\mathbf{t}_1(X) = \mathbf{t}_2(X) \times \mathbf{t}_3(X)$  is the normal basis vector of the section, as shown in Fig. 2. The orthogonal matrices  $\mathbf{R}^g \in \text{SO}(3)$  and  $\mathbf{R} \in \text{SO}(3)$  describe the rotations from the material and spatial basis vectors to the orthonormal triads  $\mathbf{t}_i$  ( $i = 1, 2, 3$ ), respectively, i.e.

$$\mathbf{t}_i(X) = \mathbf{R}^g(X)\mathbf{E}_i = \mathbf{R}^g(X)\mathbf{R}_0\mathbf{e}_i = \mathbf{R}(X)\mathbf{e}_i, \quad i = 1, 2, 3 \quad (3)$$

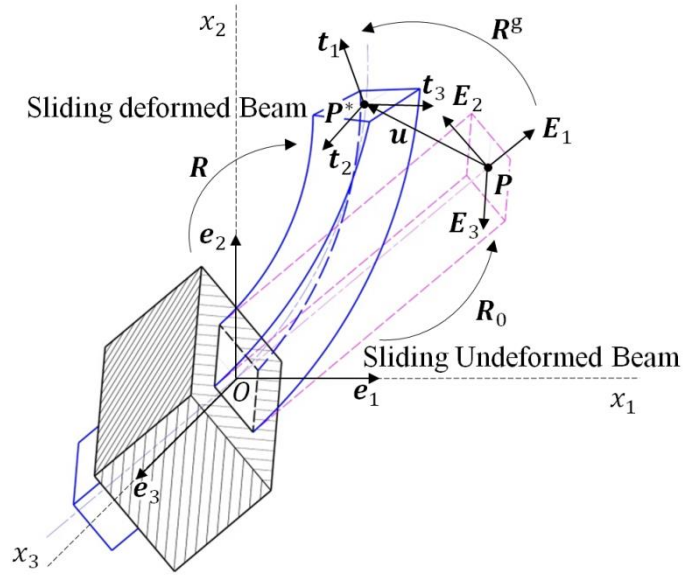


**Fig. 2** Description of the finite deformation of the beam

The material point  $\mathbf{P}$  and the corresponding spatial point  $\mathbf{P}^* \in \mathcal{B}_s$  have the following relationship

$$\mathbf{P}^* = \mathbf{P} + \mathbf{u}(X) \quad (4)$$

where  $\mathbf{u}(X)$  denotes the displacement vector of the material point  $\mathbf{P}$ . It should be noted that  $\mathbf{u}$  is not the absolute displacement but the relative displacement to the material configuration. The material point  $\mathbf{P}_a = (X, X_2, X_3) \in \mathcal{B}_m$  has the same cross-section as the point  $\mathbf{P}$  and the corresponding spatial point  $\mathbf{P}_a^* \in \mathcal{B}_s$  satisfies

$$\mathbf{P}_a^* = \mathbf{P}^* + X_2 \mathbf{t}_2(X) + X_3 \mathbf{t}_3(X) = \mathbf{P}^* + \mathbf{R}(X)(X_2 \mathbf{e}_2 + X_3 \mathbf{e}_3) \quad (5)$$

According to Eqs. (4) and (5), the configuration space of the 3D flexible beam is a nonlinear differentiable manifold due to the introduction of  $\mathbf{R}(X)$ . The displacement vector  $\mathbf{u}(X)$  and the rotation matrix  $\mathbf{R}(X)$  of the material points of the beam centroidal line directly determine the spatial configuration of the beam. The displacement space of the beam can be defined as follows

$$\bar{\mathcal{Q}} = \{(\mathbf{u}(\mathbf{P}), \mathbf{R}(\mathbf{P})) \in \mathbb{R}^3 \times \text{SO}(3) | \mathbf{P} = (X, 0, 0) \in \mathcal{B}_m\} \quad (6)$$

Euler's theorem indicates that the rotation matrix  $\mathbf{R}$  can be parameterized using the rotational vector  $\boldsymbol{\theta} = [\theta_1 \ \theta_2 \ \theta_3]^T$ . The relation is given by Rodrigues' formula

$$\mathbf{R}(\boldsymbol{\theta}) = \mathbf{I} + \frac{\sin \theta}{\theta} \tilde{\boldsymbol{\theta}} + \frac{1 - \cos \theta}{\theta^2} \tilde{\boldsymbol{\theta}} \tilde{\boldsymbol{\theta}} = \exp(\tilde{\boldsymbol{\theta}}) \quad (7)$$

where  $\theta = \sqrt{\boldsymbol{\theta}^T \boldsymbol{\theta}}$  and  $\tilde{\boldsymbol{\theta}} \in \text{so}(3)$ .  $\text{so}(3)$  denotes the Lie algebra of  $\text{SO}(3)$  [45].

$\sim: \mathbb{R}^3 \rightarrow \text{so}(3)$  denotes the Lie algebra isomorphism, i.e.

$$\tilde{\boldsymbol{\theta}} = \begin{bmatrix} 0 & -\theta_3 & \theta_2 \\ \theta_3 & 0 & -\theta_1 \\ -\theta_2 & \theta_1 & 0 \end{bmatrix}, \quad \tilde{\boldsymbol{\theta}} \mathbf{h} = \boldsymbol{\theta} \times \mathbf{h}, \quad \forall \mathbf{h} \in \mathbb{R}^3 \quad (8)$$

The operator  $\text{vect}(\cdot)$  is defined by

$$\text{vect}(\tilde{\boldsymbol{\theta}}) = \boldsymbol{\theta} \quad (9)$$

Next, define a space  $\mathcal{Q}$  which is isomorphic to the displacement space  $\bar{\mathcal{Q}}$ , i.e.

$$\mathcal{Q} = \{(\mathbf{u}(\mathbf{P}), \boldsymbol{\theta}(\mathbf{P})) \in \mathbb{R}^3 \times \mathbb{R}^3 \mid \mathbf{P} = (X, 0, 0) \in \mathcal{B}_m\} \quad (10)$$

The part of the beam  $\mathcal{B}_m$  inside the joint channel is assumed to be non-deformable, which implies that the beam has a clamped boundary condition at the channel orifice [10, 34]. Then  $\mathbf{u}(\mathbf{P}_0) = 0$ ,  $\boldsymbol{\theta}(\mathbf{P}_0) = 0$ , where  $\mathbf{P}_0 = (0, 0, 0) \in \mathcal{B}_m$  is the material point at the channel orifice.

### 3. Local kinematic description of the variable-domain beam elements

The sliding beam can be divided into  $n$  elements with the lengths  $l_0(t) = L(t)/n$  which are changing in time. As shown in Fig. 3, the displacements of nodes 1 and 2 of the  $i$ th element can be denoted by  $(\mathbf{u}_1, \boldsymbol{\theta}_1) = (\mathbf{u}(\mathbf{P}), \boldsymbol{\theta}(\mathbf{P}))_{\mathbf{P}=(i-1)L/n, 0, 0} \in \mathcal{Q}$  and  $(\mathbf{u}_2, \boldsymbol{\theta}_2) = (\mathbf{u}(\mathbf{P}), \boldsymbol{\theta}(\mathbf{P}))_{\mathbf{P}=(iL/n, 0, 0)} \in \mathcal{Q}$ , respectively. For convenience, the subscript  $i$  of variables which are associated with the  $i$ th element will be ignored. The global

displacement vector of the  $i$ th element is defined by

$$\mathbf{q} = [\mathbf{u}_1^T \quad \boldsymbol{\theta}_1^T \quad \mathbf{u}_2^T \quad \boldsymbol{\theta}_2^T]^T \quad (11)$$

As shown in Fig. 3,  $\mathbf{t}_j^1$  and  $\mathbf{t}_j^2$  ( $j = 1,2,3$ ), denote two unit triads fixed to nodes 1 and

2. Then two orthogonal matrices  $\mathbf{R}_1$  and  $\mathbf{R}_2$  are used to specify the orientation of the

two triads, respectively,

$$\mathbf{R}_i = [\mathbf{t}_1^k \quad \mathbf{t}_2^k \quad \mathbf{t}_3^k], \quad k = 1,2 \quad (12)$$

The spatial positions of the two nodes on the material configuration are expressed as

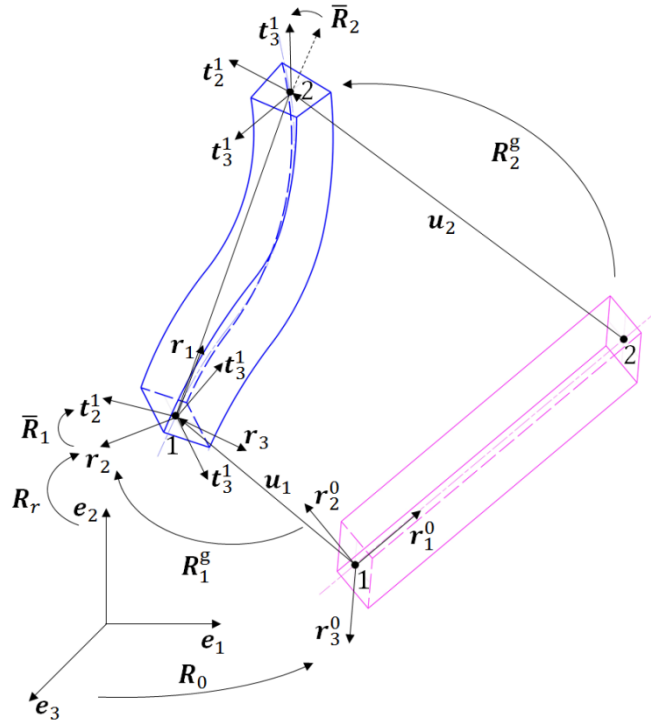


**Fig. 3** Description of the deformation of the beam element

$$\mathbf{X}_1 = (i-1)l_0\mathbf{R}_0\mathbf{e}_1, \quad \mathbf{X}_2 = il_0\mathbf{R}_0\mathbf{e}_1 \quad (13)$$

### 3.1. Corotational frame

The basis vectors of the corotational frame are denoted by  $\{\mathbf{r}_1, \mathbf{r}_2, \mathbf{r}_3\}$ . The origin of the frame is taken at node 1, and its orientation is defined by an orthogonal matrix

$$\mathbf{R}_r = [\mathbf{r}_1 \quad \mathbf{r}_2 \quad \mathbf{r}_3] \quad (14)$$

The method proposed by Le et al. [41] is used to defined the orientation of  $\mathbf{r}_1$ ,  $\mathbf{r}_2$  and  $\mathbf{r}_3$ , as follows

$$l_c = \sqrt{(\mathbf{X}_2 + \mathbf{u}_2 - \mathbf{X}_1 - \mathbf{u}_1)^T (\mathbf{X}_2 + \mathbf{u}_2 - \mathbf{X}_1 - \mathbf{u}_1)} \quad (15)$$

$$\mathbf{r}_1 = \frac{\mathbf{X}_2 + \mathbf{u}_2 - \mathbf{X}_1 - \mathbf{u}_1}{l_c} \quad (16)$$

$$\begin{aligned} \mathbf{p} &= \frac{1}{2}(\mathbf{p}_1 + \mathbf{p}_2), \\ \mathbf{p}_k &= \mathbf{R}_k [0 \quad 1 \quad 0]^T = \mathbf{R}_k^g \mathbf{R}_0 [0 \quad 1 \quad 0]^T = \mathbf{R}_k^g \mathbf{r}_2^0, \quad k = 1, 2 \end{aligned} \quad (17)$$

$$\mathbf{r}_3 = \frac{\mathbf{r}_1 \times \mathbf{p}}{\|\mathbf{r}_1 \times \mathbf{p}\|}, \quad \mathbf{r}_2 = \mathbf{r}_3 \times \mathbf{r}_1 \quad (18)$$

where  $l_c$  is the distance between the nodes and  $\mathbf{R}_k^g$  are the orthogonal matrices to describe the rotation from  $\mathbf{r}_j^0$  to  $\mathbf{t}_j^k (j = 1, 2, 3)$ .

### 3.2. Local displacement field of elements

The pure deformation of the element is measured in the rotational frame. Due to the particular choice of the local system, the local displacements at node 1 are zero. Moreover,

at node 2, the only nonzero displacement is along  $\mathbf{r}_1$  and can easily be evaluated according to

$$\bar{u} = l_c - l_0 \quad (19)$$

Here and hereafter, an overbar denotes a deformational kinematic quantity.

The local rotation is defined by the orthogonal matrix  $\bar{\mathbf{R}}_k$ , as shown in Fig. 3. The global rotation  $\mathbf{R}_k$  at node  $k$  can be expressed in terms of the rigid rotation  $\mathbf{R}_r$  of the corotational frame followed by the local rotation  $\bar{\mathbf{R}}_k$ . As shown in Fig. 3,  $\mathbf{R}_k$  can also be obtained through the product  $\mathbf{R}_k^g \mathbf{R}_0$ , i.e.,

$$\mathbf{R}_k = \mathbf{R}_r \bar{\mathbf{R}}_k = \mathbf{R}_k^g \mathbf{R}_0, \quad k = 1, 2 \quad (20)$$

The local rotation  $\bar{\mathbf{R}}_k$  can be parameterized using a rotational vector from Eqs. (7)-(9).

Consequently, we can define a local displacement vector with seven components, i.e.,

$$\bar{\mathbf{q}} = [\bar{u} \quad \bar{\boldsymbol{\theta}}_1^T \quad \bar{\boldsymbol{\theta}}_2^T]^T \quad (21)$$

where

$$\bar{\boldsymbol{\theta}}_k = \text{vect}(\ln(\bar{\mathbf{R}}_k)), \quad k = 1, 2 \quad (22)$$

To consider the shear deformation and rotary inertia, the IIE [42], which is locking-free, is used to describe the local displacement field of the element. The shape functions

of this element are based on the exact solution of homogeneous form of the equilibrium equations for a Timoshenko beam. It should be noted that this exact solution is based on linear theory. The element should be small enough to ensure that only small deformations occur in the local system. Let  $\bar{\bar{u}}_i(\chi)(i = 1, 2, 3)$  and  $\bar{\bar{\theta}}_i(\chi)(i = 1, 2, 3)$  denote the local displacements and the local cross-section rotations of a material point with local coordinate  $\chi$ . A double overbar denotes a local kinematic quantity of an arbitrary material point. Considering the particular choice of the local displacement vector  $\bar{\mathbf{q}}$ , the local displacement field of the element can be expressed as [42]

$$\begin{bmatrix} \bar{\bar{u}}_1 \\ \bar{\bar{u}}_2 \\ \bar{\bar{u}}_3 \\ \bar{\bar{\theta}}_1 \\ \bar{\bar{\theta}}_2 \\ \bar{\bar{\theta}}_3 \end{bmatrix} = \begin{bmatrix} N_2 & 0 & 0 & 0 & 0 & 0 & 0 \\ 0 & 0 & 0 & N_3^3 & 0 & 0 & N_4^3 \\ 0 & 0 & -N_3^2 & 0 & 0 & -N_4^2 & 0 \\ 0 & N_1 & 0 & 0 & N_2 & 0 & 0 \\ 0 & 0 & N_5^2 & 0 & 0 & N_6^2 & 0 \\ 0 & 0 & 0 & N_5^3 & 0 & 0 & N_6^3 \end{bmatrix} \bar{\mathbf{q}} \quad (23)$$

where

$$\begin{aligned} N_1 &= 1 - \frac{\chi}{l_0}, \quad N_2 = \frac{\chi}{l_0}, \quad N_3^j = \frac{1}{\mu_j} \chi \left[ 6\Omega_j \left( 1 - \frac{\chi}{l_0} \right) + \left( 1 - \frac{\chi}{l_0} \right)^2 \right], \\ N_4^j &= -\frac{1}{\mu_j} \chi \left[ 6\Omega_j \left( 1 - \frac{\chi}{l_0} \right) + \frac{\chi}{l_0} - \frac{\chi^2}{l_0^2} \right], \\ N_5^j &= \frac{1}{\mu_j} \left( \mu_j - \frac{12\Omega_j \chi}{l_0} - \frac{4\chi}{l_0} + \frac{3\chi^2}{l_0^2} \right), \\ N_6^j &= \frac{1}{\mu_j} \left( \frac{12\Omega_j \chi}{l_0} - \frac{2\chi}{l_0} + \frac{3\chi^2}{l_0^2} \right), \quad \Omega_j = \frac{EI_j}{GA_j l_0^2}, \\ \mu_j &= 1 + 12\Omega_j, \quad j = 2, 3 \end{aligned} \quad (24)$$



Here,  $EI_j$  is the principal bending stiffness relative to  $\mathbf{t}_j$  and  $GA_j$  is the shear stiffness along axis  $\mathbf{t}_j$  ( $j = 2,3$ ). The local coordinate  $\chi$  and the material coordinate  $X$  have the following relationship:

$$\chi = X - (i - 1)l_0 \quad (25)$$

### 3.3. Local elastic force vector and Local tangent stiffness matrix

To consider the axial deformation, bending deformation and shear deformation of the beam, the strain energy of a beam element can be expressed as [23]

$$E_p = \frac{1}{2} \int_{l_0} \boldsymbol{\kappa} \mathbf{C} \boldsymbol{\kappa}^T d\chi \quad (26)$$

The strain vector  $\boldsymbol{\kappa}$  and elasticity matrix  $\mathbf{C}$  are given by

$$\boldsymbol{\kappa} = \begin{bmatrix} \frac{\partial \bar{u}_1}{\partial \chi} & -\frac{\partial \bar{u}_3}{\partial \chi} - \bar{\theta}_2 & \frac{\partial \bar{u}_2}{\partial \chi} - \bar{\theta}_3 & \frac{\partial \bar{\theta}_1}{\partial \chi} & \frac{\partial \bar{\theta}_2}{\partial \chi} & \frac{\partial \bar{\theta}_3}{\partial \chi} \end{bmatrix} \quad (27)$$

$$\mathbf{C} = \text{diag}[EA, GA_2, GA_3, GJ, EI_2, EI_3] \quad (28)$$

where  $EA$  and  $GJ$  are the axial stiffness and torsional stiffness, respectively. Using Eqs.

(23)-(28), the local elastic force vector and tangent stiffness matrix are obtained as

$$\mathbf{f}_L = \frac{\partial E_p}{\partial \bar{\mathbf{q}}} = \mathbf{K}_L \bar{\mathbf{q}} = [f_{L1} \quad f_{L2} \quad f_{L3} \quad f_{L4} \quad f_{L5} \quad f_{L6} \quad f_{L7}]^T \quad (29)$$

$$\mathbf{K}_L = \frac{\partial \mathbf{f}_L}{\partial \mathbf{q}} = \begin{bmatrix} \frac{EA}{l_0} & 0 & 0 & 0 & 0 & 0 & 0 \\ 0 & \frac{GJ}{l_0} & 0 & 0 & -\frac{GJ}{l_0} & 0 & 0 \\ 0 & 0 & \frac{4\lambda_{12}}{\mu_2^2 l_0} & 0 & 0 & \frac{2\lambda_{22}}{\mu_2^2 l_0} & 0 \\ 0 & 0 & 0 & 0 & 0 & 0 & 0 \\ 0 & 0 & 0 & \frac{4\lambda_{13}}{\mu_3^2 l_0} & 0 & 0 & \frac{2\lambda_{23}}{\mu_3^2 l_0} \\ 0 & -\frac{GJ}{l_0} & 0 & 0 & \frac{GJ}{l_0} & 0 & 0 \\ 0 & 0 & \frac{2\lambda_{22}}{\mu_2^2 l_0} & 0 & 0 & \frac{4\lambda_{12}}{\mu_2^2 l_0} & 0 \\ 0 & 0 & 0 & \frac{2\lambda_{23}}{\mu_3^2 l_0} & 0 & 0 & \frac{4\lambda_{13}}{\mu_3^2 l_0} \end{bmatrix} \quad (30)$$

where

$$\begin{aligned} \lambda_{1j} &= 9GA_j l_0^2 \Omega_j^2 + 36EI_j \Omega_j^2 + 6EI_j \Omega_j + EI_j, \\ \lambda_{2j} &= 18GA_j l_0^2 \Omega_j^2 - 72EI_j \Omega_j^2 - 12EI_j \Omega_j + EI_j, \quad j = 2, 3 \end{aligned} \quad (31)$$

#### 4. Nonlinear equation of motion

According to the analysis in [1, 46], the Hamilton's principle for a system of changing mass [7] can be expressed as

$$\delta \int_{t_1}^{t_2} (E_K - E_P) dt + \int_{t_1}^{t_2} \delta W dt = 0 \quad (32)$$

The kinetic energy  $E_K$  of a beam element can be expressed as

$$E_K = \frac{1}{2} \int_{l_0} (\dot{\mathbf{u}}_g^T \mathbf{A}_\rho \dot{\mathbf{u}}_g + \dot{\mathbf{w}}_g^T \mathbf{I}_\rho \dot{\mathbf{w}}_g) d\chi \quad (33)$$

where  $\dot{\mathbf{u}}_g$  and  $\dot{\mathbf{w}}_g$  are the translational velocity and the spatial angular velocity of the cross-section.  $A_\rho$  is the mass per unit of undeformed beam length.  $\mathbf{I}_\rho$  is the spatial inertia dyadic tensor defined as

$$\mathbf{I}_\rho = \mathbf{R} \mathbf{J}_\rho \mathbf{R}^T \quad (34)$$

where  $\mathbf{J}_\rho$  is the material inertia dyadic tensor (constant with respect to time). The virtual work of the external forces is

$$\delta W = \delta \mathbf{q}_g^T \mathbf{f} \quad (35)$$

where  $\mathbf{f}$  denotes the external force vector.

#### 4.1. Elastic force vector

This section is devoted to the derivation of the elastic force vector. The term  $\delta \int_{t_1}^{t_2} E_P dt$  in Eq. (32) can be expressed in the global and local systems, respectively, i.e.

$$\delta \int_{t_1}^{t_2} E_P dt = \int_{t_1}^{t_2} \delta \mathbf{q}_g^T \mathbf{f}_G dt = \int_{t_1}^{t_2} \delta \bar{\mathbf{q}}^T \mathbf{f}_L dt \quad (36)$$

where  $\mathbf{f}_G$  denotes the global elastic force vector.  $\delta \mathbf{q}_g^T$  and  $\delta \bar{\mathbf{q}}^T$  are defined by

$$\delta \mathbf{q}_g = [\delta \mathbf{u}_1^T \quad \delta \mathbf{w}_1^{gT} \quad \delta \mathbf{u}_2^T \quad \delta \mathbf{w}_2^{gT}]^T \quad (37)$$

$$\delta \bar{\mathbf{q}} = [\delta \bar{\mathbf{u}} \quad \delta \bar{\mathbf{w}}_1^T \quad \delta \bar{\mathbf{w}}_2^T]^T \quad (38)$$

It should be noted that  $\delta \mathbf{w}_k^g (k = 1, 2)$  are non-additive pseudo-vectors. The non-additive  $(\delta \mathbf{w}_k)$  and additive  $(\delta \boldsymbol{\theta}_k)$  pseudo-vectors (as defined in Eq. (11)) have the following relationship [44]:

$$\delta \mathbf{w}_k^g = \mathbf{T}(\boldsymbol{\theta}_k) \delta \boldsymbol{\theta}_k, \quad k = 1, 2 \quad (39)$$

where the operator  $\mathbf{T}(\boldsymbol{\theta})$  is defined (using  $\boldsymbol{\theta}$  as an example) by

$$\mathbf{T}(\boldsymbol{\theta}) = \frac{\sin \theta}{\theta} \mathbf{I} + \frac{1 - \cos \theta}{\theta^2} \tilde{\boldsymbol{\theta}} + \frac{\theta - \sin \theta}{\theta^3} \tilde{\boldsymbol{\theta}} \tilde{\boldsymbol{\theta}} \quad (40)$$

Considering the local rotation is assumed to be small [41, 47] and using Eq. (40), the following approximation is adopted

$$\delta \bar{\mathbf{w}}_k = \mathbf{T}(\bar{\boldsymbol{\theta}}_k) \delta \bar{\boldsymbol{\theta}}_k \approx \delta \bar{\boldsymbol{\theta}}_k, \quad k = 1, 2 \quad (41)$$

The following derivation is to establish a relationship between  $\delta \mathbf{q}_g^T$  and  $\delta \bar{\mathbf{q}}^T$ . Then, the global elastic force vector  $\mathbf{f}_G$  will be obtained by using Eq. (36). First, we will investigate the component  $\delta \bar{u}$  in  $\delta \bar{\mathbf{q}}^T$ .

Since the beam is manipulated by the revolute-prismatic joint, the prescribed orthogonal matrix  $\mathbf{R}_0$  as defined in Eq. (2) and the element length  $l_0$  are functions of time. By taking the variation of Eq. (13), one obtains

$$\delta \mathbf{X}_1 = (\nu \mathbf{R}_0 + L \dot{\mathbf{R}}_0) \frac{i-1}{n} \mathbf{e}_1 \delta t, \quad \delta \mathbf{X}_2 = (\nu \mathbf{R}_0 + L \dot{\mathbf{R}}_0) \frac{i}{n} \mathbf{e}_1 \delta t \quad (42)$$

where  $v = dL/dt = dX/dt$  denotes the sliding speed of the beam. It should be pointed out that  $\mathbf{R}_0$ ,  $\dot{\mathbf{R}}_0$ ,  $L$  and  $v$  are prescribed according to the manipulation of the revolute-prismatic joint. Using Eq. (42) and taking the variation of Eqs. (15) and (19), one obtains

$$\delta l_c = \bar{\mathbf{U}} \delta \mathbf{q}_g + \left( \frac{v}{n} \mathbf{r}_1^{0T} \mathbf{r}_1 + l_0 \dot{\mathbf{r}}_1^{0T} \mathbf{r}_1 \right) \delta t \quad (43)$$

$$\delta \bar{u} = \bar{\mathbf{U}} \delta \mathbf{q}_g + \left[ \frac{v}{n} \left( \mathbf{r}_1^{0T} \mathbf{r}_1 - 1 \right) + l_0 \dot{\mathbf{r}}_1^{0T} \mathbf{r}_1 \right] \delta t \quad (44)$$

where

$$\bar{\mathbf{U}} = [-\mathbf{r}_1^T \quad \mathbf{0}_{1 \times 3} \quad \mathbf{r}_1^T \quad \mathbf{0}_{1 \times 3}] \quad (45)$$

Next, we will investigate the components  $\delta \bar{\mathbf{w}}_1$  and  $\delta \bar{\mathbf{w}}_2$  in  $\delta \bar{\mathbf{q}}^T$ . The variations of  $\bar{\mathbf{R}}_k$ ,  $\mathbf{R}_r$  and  $\mathbf{R}_k^g$  can be expressed as [44]

$$\delta \bar{\mathbf{R}}_k = \delta \widetilde{\mathbf{w}}_k \bar{\mathbf{R}}_k, \quad \delta \mathbf{R}_r = \delta \widetilde{\mathbf{w}}_r^g \mathbf{R}_r, \quad \delta \mathbf{R}_k^g = \delta \widetilde{\mathbf{w}}_k^g \mathbf{R}_k^g, \quad k = 1, 2 \quad (46)$$

The orthogonal matrix  $\mathbf{R}_r$  transforms a vector  $\mathbf{x}^g$  and a tensor  $\widetilde{\mathbf{x}}^g$  from global to local coordinates according to

$$\mathbf{x}^e = \mathbf{R}_r^T \mathbf{x}^g, \quad \widetilde{\mathbf{x}}^e = \mathbf{R}_r^T \widetilde{\mathbf{x}}^g \mathbf{R}_r \quad (47)$$

Considering the property of the Lie algebra isomorphism  $\widetilde{\cdot}^T = -\widetilde{\cdot}$  and using Eqs. (20) and (46),  $\delta \bar{\mathbf{R}}_k$  can be further expressed as

$$\begin{aligned}
\delta \bar{\mathbf{R}}_k &= \delta \mathbf{R}_r^T \mathbf{R}_k^g \mathbf{R}_0 + \mathbf{R}_r^T \delta \mathbf{R}_k^g \mathbf{R}_0 + \mathbf{R}_r^T \mathbf{R}_k^g \delta \mathbf{R}_0 \\
&= \left( -\mathbf{R}_r^T \delta \widetilde{\mathbf{w}}_r^g \mathbf{R}_r + \mathbf{R}_r^T \delta \widetilde{\mathbf{w}}_k^g \mathbf{R}_r \right) \bar{\mathbf{R}}_k + \mathbf{R}_r^T \mathbf{R}_k^g \dot{\mathbf{R}}_0 \mathbf{R}_0^T \mathbf{R}_k^g \mathbf{R}_r \delta t \bar{\mathbf{R}}_k \quad (48) \\
&= \left( -\mathbf{R}_r^T \delta \widetilde{\mathbf{w}}_r^g \mathbf{R}_r + \mathbf{R}_r^T \delta \widetilde{\mathbf{w}}_k^g \mathbf{R}_r + \bar{\mathbf{R}}_k \mathbf{R}_0^T \dot{\mathbf{R}}_0 \bar{\mathbf{R}}_k^T \delta t \right) \bar{\mathbf{R}}_k
\end{aligned}$$

As in Eq. (47), following definitions are introduced:

$$\begin{aligned}
\delta \widetilde{\mathbf{w}}_k^e &= \mathbf{R}_r^T \delta \widetilde{\mathbf{w}}_k^g \mathbf{R}_r \\
\delta \widetilde{\mathbf{w}}_r^e &= \mathbf{R}_r^T \delta \widetilde{\mathbf{w}}_r^g \mathbf{R}_r \\
\delta \widetilde{\mathbf{w}}_0^k &= \bar{\mathbf{R}}_k \mathbf{R}_0^T \dot{\mathbf{R}}_0 \bar{\mathbf{R}}_k^T \delta t
\end{aligned} \quad (49)$$

Inserting Eq. (49) into Eq. (48) and using Eq. (46),  $\delta \widetilde{\mathbf{w}}_k$  can be expressed in vector form,

i.e.,

$$\delta \bar{\mathbf{w}}_k = \delta \mathbf{w}_k^e - \delta \mathbf{w}_r^e + \dot{\mathbf{w}}_0^k \delta t \quad (50)$$

where

$$\dot{\mathbf{w}}_0^k = \text{vect}(\bar{\mathbf{R}}_k \mathbf{R}_0^T \dot{\mathbf{R}}_0 \bar{\mathbf{R}}_k^T) = \bar{\mathbf{R}}_k \text{vect}(\mathbf{R}_0^T \dot{\mathbf{R}}_0) \quad (51)$$

As shown in Eq. (15),  $\delta \bar{\mathbf{w}}_k$  is related to  $\delta \mathbf{w}_k^e$  and  $\delta \mathbf{w}_r^e$ . Next, we will investigate these

two terms. Let

$$\delta \mathbf{q}_g^e = \mathbf{E}^T \delta \mathbf{q}_g, \quad \mathbf{E} = \begin{bmatrix} \mathbf{R}_r & \mathbf{0} & \mathbf{0} & \mathbf{0} \\ \mathbf{0} & \mathbf{R}_r & \mathbf{0} & \mathbf{0} \\ \mathbf{0} & \mathbf{0} & \mathbf{R}_r & \mathbf{0} \\ \mathbf{0} & \mathbf{0} & \mathbf{0} & \mathbf{R}_r \end{bmatrix} \quad (52)$$

with  $\mathbf{0}$  denoting the  $3 \times 3$  zero matrix. Further, the term  $\delta \mathbf{w}_k^e (k = 1, 2)$  in Eq. (50)

can be rewritten as

$$\begin{bmatrix} \delta \mathbf{w}_1^e \\ \delta \mathbf{w}_2^e \end{bmatrix} = \frac{\partial \mathbf{w}_r^e}{\partial \mathbf{q}_g^e} \frac{\partial \mathbf{q}_g^e}{\partial \mathbf{q}_g} \delta \mathbf{q}_g = \begin{bmatrix} \mathbf{0} & \mathbf{I} & \mathbf{0} & \mathbf{0} \\ \mathbf{0} & \mathbf{0} & \mathbf{0} & \mathbf{I} \end{bmatrix} \mathbf{E}^T \delta \mathbf{q}_g \quad (53)$$

Next, the relationships between  $\delta \mathbf{w}_k^e (k = 1, 2)$  and  $\delta \mathbf{q}_g$  are obtained.

From Eqs. (46) and (47), one obtains

$$\widetilde{\delta \mathbf{w}}_r^e = \mathbf{R}_r^T \delta \mathbf{R}_r, \quad \delta \mathbf{w}_r^e = \text{vect}(\mathbf{R}_r^T \delta \mathbf{R}_r) = \begin{bmatrix} -\mathbf{r}_2^T \delta \mathbf{r}_3 \\ -\mathbf{r}_3^T \delta \mathbf{r}_1 \\ \mathbf{r}_2^T \delta \mathbf{r}_1 \end{bmatrix} \quad (54)$$

with  $-\mathbf{r}_2^T \delta \mathbf{r}_3$ ,  $-\mathbf{r}_3^T \delta \mathbf{r}_1$  and  $\mathbf{r}_2^T \delta \mathbf{r}_1$  given in [Appendix A](#). Inserting these terms into Eq.

(54), one obtains

$$\delta \mathbf{w}_r^e = \mathbf{G}_1^T \mathbf{E}^T \delta \mathbf{q}_g + \mathbf{G}_2^T \delta t \quad (55)$$

where

$$\mathbf{G}_1^T = \begin{bmatrix} 0 & 0 & \frac{\eta}{l_c} & \frac{\eta_{12}}{2} & -\frac{\eta_{11}}{2} & 0 & 0 & 0 & -\frac{\eta}{l_c} & \frac{\eta_{22}}{2} & -\frac{\eta_{21}}{2} & 0 \\ 0 & 0 & \frac{1}{l_c} & 0 & 0 & 0 & 0 & 0 & -\frac{1}{l_c} & 0 & 0 & 0 \\ 0 & -\frac{1}{l_c} & 0 & 0 & 0 & 0 & 0 & \frac{1}{l_c} & 0 & 0 & 0 & 0 \end{bmatrix} \quad (56)$$

with

$$\eta = \frac{\mathbf{r}_1 \cdot \mathbf{p}}{\mathbf{r}_2 \cdot \mathbf{p}}, \quad \eta_{ij} = \frac{\mathbf{r}_j \cdot \mathbf{p}_i}{\mathbf{r}_2 \cdot \mathbf{p}}, \quad i, j = 1, 2 \quad (57)$$

and

$$\mathbf{G}_2^T = \begin{bmatrix} \frac{-(\mathbf{r}_1^T \mathbf{p}) \mathbf{e}_3^T \mathbf{R}_r^T \frac{v \mathbf{r}_1^0 + L \dot{\mathbf{r}}_1^0}{n l_c} + \mathbf{e}_3^T \frac{\bar{\mathbf{R}}_1 + \bar{\mathbf{R}}_2}{2} \mathbf{R}_0^T \dot{\mathbf{r}}_2^0}{\mathbf{r}_2^T \mathbf{p}} \\ -\mathbf{e}_3^T \mathbf{R}_r^T \frac{v \mathbf{r}_1^0 + L \dot{\mathbf{r}}_1^0}{n l_c} \\ -\mathbf{e}_2^T \mathbf{R}_r^T \frac{v \mathbf{r}_1^0 + L \dot{\mathbf{r}}_1^0}{n l_c} \end{bmatrix} = \begin{bmatrix} G_2^1 \\ G_2^2 \\ G_2^3 \end{bmatrix} \quad (58)$$

Inserting Eqs. (53) and (55) into Eq. (50),

$$\begin{aligned} \begin{bmatrix} \delta \bar{\mathbf{w}}_1 \\ \delta \bar{\mathbf{w}}_2 \end{bmatrix} &= \left( \begin{bmatrix} \mathbf{0} & \mathbf{I} & \mathbf{0} & \mathbf{0} \\ \mathbf{0} & \mathbf{0} & \mathbf{0} & \mathbf{I} \end{bmatrix} - \begin{bmatrix} \mathbf{G}_1^T \\ \mathbf{G}_2^T \end{bmatrix} \right) \mathbf{E}^T \delta \mathbf{q}_g + \begin{bmatrix} -\mathbf{G}_2^T + \dot{\mathbf{w}}_0^1 \\ -\mathbf{G}_2^T + \dot{\mathbf{w}}_0^2 \end{bmatrix} \delta t \\ &= \mathbf{P}_1 \mathbf{E}^T \delta \mathbf{q}_g + \mathbf{P}_2 \delta t \end{aligned} \quad (59)$$

Further, inserting Eqs. (44) and (59) into Eq. (38),  $\delta \bar{\mathbf{q}}$  can be rewritten as

$$\delta \bar{\mathbf{q}} = \mathbf{B}_1 \delta \mathbf{q}_g + \mathbf{B}_2 \delta t \quad (60)$$

where

$$\mathbf{B}_1 = \begin{bmatrix} \bar{\mathbf{U}} \\ \mathbf{P}_1 \mathbf{E}^T \end{bmatrix}, \quad \mathbf{B}_2 = \begin{bmatrix} v \left( \mathbf{r}_1^{0T} \mathbf{r}_1 - 1 \right) + L \dot{\mathbf{r}}_1^{0T} \mathbf{r}_1 \\ n \\ \mathbf{P}_2 \end{bmatrix} \quad (61)$$

Finally, by inserting Eq. (60) into Eq. (36) the relationship between the global and local elastic force vector is obtained, i.e.

$$\mathbf{f}_G = \mathbf{B}_1^T \mathbf{f}_L \quad (62)$$



## 4.2. Inertia force vector

This section is devoted to the derivation of the inertia force vector. The material angular velocity is defined by

$$\boldsymbol{\Omega} = \mathbf{R}^T \dot{\mathbf{w}}_g, \quad \widetilde{\boldsymbol{\Omega}} = \mathbf{R}^T \dot{\mathbf{R}} = \mathbf{R}^T \widetilde{\dot{\mathbf{w}}_g} \mathbf{R} \quad (63)$$

with  $\mathbf{R}$  as defined in Eq. (3). The kinetic energy of the element can be rewritten in the material form, i.e.

$$E_K = \frac{1}{2} \int_{l_0} (\dot{\mathbf{u}}_g^T A_\rho \dot{\mathbf{u}}_g + \boldsymbol{\Omega}^T \mathbf{J}_\rho \boldsymbol{\Omega}) d\chi \quad (64)$$

Inserting Eq. (64) into Eq. (32) and integrating  $\delta \int_{t_1}^{t_2} E_K dt$  by parts, one obtains (see [48] for detailed derivations)

$$\begin{aligned} \delta \int_{t_1}^{t_2} E_K dt &= - \int_{t_1}^{t_2} \int_{l_0} \left( \delta \mathbf{u}_g^T A_\rho \ddot{\mathbf{u}}_g + \delta \boldsymbol{\theta}^T (\mathbf{J}_\rho \dot{\boldsymbol{\Omega}} + \widetilde{\boldsymbol{\Omega}} \mathbf{J}_\rho \boldsymbol{\Omega}) \right) d\chi dt \\ &= - \int_{t_1}^{t_2} \delta \mathbf{q}_g^T \mathbf{f}_I dt \end{aligned} \quad (65)$$

where  $\mathbf{f}_I$  denotes the inertia force vector and  $\delta \boldsymbol{\theta}$  is the material spin variable defined by

$$\delta \boldsymbol{\theta} = \mathbf{R}^T \delta \mathbf{w}_g, \quad \widetilde{\delta \boldsymbol{\theta}} = \mathbf{R}^T \delta \mathbf{R} \quad (66)$$

The translational displacement variables and finite rotation variables in Eq. (65) will

now be derived. First, we consider the translational displacement variables. The spatial position of the material point  $\mathbf{P} = ((i-1)L/n + \chi, 0, 0)$  on the  $i$ th element can be expressed as

$$\begin{aligned}\mathbf{P}_g &= \mathbf{X}_1 + \mathbf{u}_1 + (\chi + \bar{u}_1)\mathbf{r}_1 + \bar{u}_2\mathbf{r}_2 + \bar{u}_3\mathbf{r}_3 \\ &= N_1\mathbf{X}_1 + N_2\mathbf{X}_2 + N_1\mathbf{q}_g + \mathbf{R}_r\mathbf{u}_l\end{aligned}\tag{67}$$

where

$$\mathbf{N}_1 = [N_1\mathbf{I} \quad \mathbf{0} \quad N_2\mathbf{I} \quad \mathbf{0}]\tag{68}$$

$$\mathbf{u}_l = N_2 \begin{bmatrix} \bar{\theta}_1 \\ \bar{\theta}_2 \end{bmatrix}\tag{69}$$

with

$$\mathbf{N}_2 = \begin{bmatrix} 0 & 0 & 0 & 0 & 0 & 0 \\ 0 & 0 & N_3^3 & 0 & 0 & N_4^3 \\ 0 & -N_3^2 & 0 & 0 & -N_4^2 & 0 \end{bmatrix}\tag{70}$$

The shape functions in Eqs. (67)-(70) are given by Eq. (24). By taking the derivation of Eq. (66), one obtains

$$\delta\mathbf{P}_g = \delta\mathbf{u}_g = \mathbf{H}_1\delta t + \mathbf{R}_r\mathbf{H}_2\mathbf{E}^T\delta\mathbf{q}_g\tag{71}$$

with  $\mathbf{H}_1$  and  $\mathbf{H}_2$  given in [Appendix B](#). Obviously, the translational velocity and acceleration of the material point can be evaluated from

$$\dot{\mathbf{u}}_g = \mathbf{H}_1 + \mathbf{R}_r \mathbf{H}_2 \mathbf{E}^T \dot{\mathbf{q}}_g \quad (72)$$

$$\ddot{\mathbf{u}}_g = \dot{\mathbf{H}}_1 + \mathbf{R}_r (\widetilde{\dot{\mathbf{w}}}_r^e \mathbf{H}_2 + \dot{\mathbf{H}}_2 - \mathbf{H}_2 \dot{\mathbf{E}}_r) \mathbf{E}^T \dot{\mathbf{q}}_g + \mathbf{R}_r \mathbf{H}_2 \mathbf{E}^T \ddot{\mathbf{q}}_g \quad (73)$$

with  $\dot{\mathbf{q}}_g = [\dot{\mathbf{u}}_1^T \quad \dot{\mathbf{w}}_1^T \quad \dot{\mathbf{u}}_2^T \quad \dot{\mathbf{w}}_2^T]^T$  and  $\ddot{\mathbf{q}}_g = [\ddot{\mathbf{u}}_1^T \quad \ddot{\mathbf{w}}_1^T \quad \ddot{\mathbf{u}}_2^T \quad \ddot{\mathbf{w}}_2^T]^T$ .  $\dot{\mathbf{H}}_1$ ,  $\dot{\mathbf{H}}_2$ ,  $\dot{\mathbf{R}}_r$  and  $\dot{\mathbf{E}}_r$  are given in [Appendix B](#).

Next, we consider the finite rotation variables. The local cross-section rotation can be expressed as

$$\bar{\boldsymbol{\theta}} = \mathbf{N}_3 \begin{bmatrix} \bar{\boldsymbol{\theta}}_1 \\ \bar{\boldsymbol{\theta}}_2 \end{bmatrix} \quad (74)$$

with

$$\mathbf{N}_3 = \begin{bmatrix} N_1 & 0 & 0 & N_2 & 0 & 0 \\ 0 & N_5^2 & 0 & 0 & N_6^2 & 0 \\ 0 & 0 & N_5^3 & 0 & 0 & N_6^3 \end{bmatrix} \quad (75)$$

Using Eqs. (47) and (50), the variation of the spatial spin  $\mathbf{w}_g$  is evaluated as [\[41\]](#)

$$\delta \mathbf{w}_g = \mathbf{R}_r (\delta \mathbf{w}_r^e + \delta \bar{\mathbf{w}}) \quad (76)$$

With the approximation adopted in Eq. (41) and using Eq. (59), the variation of Eq. (74) can be evaluated using

$$\delta \bar{\mathbf{w}} \approx \delta \bar{\boldsymbol{\theta}} = \mathbf{N}_3 \mathbf{P}_1 \mathbf{E}^T \delta \mathbf{q}_g + \left( \dot{\mathbf{N}}_3 \begin{bmatrix} \bar{\boldsymbol{\theta}}_1 \\ \bar{\boldsymbol{\theta}}_2 \end{bmatrix} + \mathbf{N}_3 \mathbf{P}_2 \right) \delta t \quad (77)$$

Then inserting Eqs. (55) and (77) into Eq. (76),  $\delta \mathbf{w}_g$  can be rewritten as

$$\delta \mathbf{w}_g = \mathbf{R}_r \mathbf{H}_3 \mathbf{E}^T \delta \mathbf{q}_g + \mathbf{R}_r \mathbf{H}_4 \delta t \quad (78)$$

where

$$\mathbf{H}_3 = \mathbf{G}_1^T + \mathbf{N}_3 \mathbf{P}_1 = \frac{1}{l_c} \left( \mathbf{I} - \mathbf{N}_3 \begin{bmatrix} \mathbf{I} \\ \mathbf{I} \end{bmatrix} \right) \mathbf{N}_4 + \mathbf{N}_3 \begin{bmatrix} \mathbf{0} & \mathbf{I} & \mathbf{0} & \mathbf{0} \\ \mathbf{0} & \mathbf{0} & \mathbf{0} & \mathbf{I} \end{bmatrix} \quad (79)$$

$$\mathbf{H}_4 = \mathbf{G}_2^T + \dot{\mathbf{N}}_3 \begin{bmatrix} \bar{\boldsymbol{\theta}}_1 \\ \bar{\boldsymbol{\theta}}_2 \end{bmatrix} + \mathbf{N}_3 \mathbf{P}_2 \quad (80)$$

with  $\mathbf{N}_4$  given in [Appendix B](#) (B.20). Then the spatial angular velocity  $\dot{\mathbf{w}}_g$  and acceleration  $\ddot{\mathbf{w}}_g$  have the following expressions

$$\dot{\mathbf{w}}_g = \mathbf{R}_r \dot{\mathbf{w}}_e, \quad \dot{\mathbf{w}}_e = \mathbf{H}_3 \mathbf{E}^T \dot{\mathbf{q}}_g + \mathbf{H}_4 \quad (81)$$

$$\begin{aligned} \ddot{\mathbf{w}}_g &= \mathbf{R}_r \ddot{\mathbf{w}}_e, \\ \ddot{\mathbf{w}}_e &= (\widetilde{\dot{\mathbf{w}}_r^e} \mathbf{H}_3 + \dot{\mathbf{H}}_3 - \mathbf{H}_3 \dot{\mathbf{E}}_r) \mathbf{E}^T \dot{\mathbf{q}}_g + \mathbf{H}_3 \mathbf{E}^T \ddot{\mathbf{q}}_g + \widetilde{\dot{\mathbf{w}}_r^e} \mathbf{H}_4 + \dot{\mathbf{H}}_4 \end{aligned} \quad (82)$$

It should be noted that  $\dot{\mathbf{w}}_e$  and  $\ddot{\mathbf{w}}_e$  are defined for convenience. The time derivative of  $\dot{\mathbf{w}}_e$  is not equal to  $\ddot{\mathbf{w}}_e$ . By taking the time derivative of Eqs. (79) and (80), one obtains

$$\begin{aligned} \dot{\mathbf{H}}_3 &= \dot{\mathbf{G}}_1^T + \mathbf{N}_3 \dot{\mathbf{P}}_1 + \dot{\mathbf{N}}_3 \mathbf{P}_1 = \dot{\mathbf{G}}_1^T - \mathbf{N}_3 \begin{bmatrix} \dot{\mathbf{G}}_1^T \\ \dot{\mathbf{G}}_1^T \end{bmatrix} + \dot{\mathbf{N}}_3 \mathbf{P}_1 \\ &= \frac{\dot{l}_c}{l_c^2} \left( \mathbf{N}_3 \begin{bmatrix} \mathbf{I} \\ \mathbf{I} \end{bmatrix} - \mathbf{I} \right) \mathbf{N}_4 + \dot{\mathbf{N}}_3 \left( \begin{bmatrix} \mathbf{0} & \mathbf{I} & \mathbf{0} & \mathbf{0} \\ \mathbf{0} & \mathbf{0} & \mathbf{0} & \mathbf{I} \end{bmatrix} - \frac{1}{l_c} \begin{bmatrix} \mathbf{I} \\ \mathbf{I} \end{bmatrix} \mathbf{N}_4 \right) \end{aligned} \quad (83)$$

$$\dot{\mathbf{H}}_4 = \dot{\mathbf{G}}_2^T + \mathbf{N}_3 \dot{\mathbf{P}}_2 + \dot{\mathbf{N}}_3 \begin{bmatrix} \bar{\boldsymbol{\theta}}_1 \\ \bar{\boldsymbol{\theta}}_2 \end{bmatrix} + \dot{\mathbf{N}}_3 \mathbf{P}_1 \mathbf{E}^T \dot{\mathbf{q}}_g + 2 \dot{\mathbf{N}}_3 \mathbf{P}_2 \quad (84)$$

By noting that  $\dot{\mathbf{R}}^T \dot{\mathbf{w}} = \mathbf{0}$  and taking the time derivative of Eq. (63), one obtains

$$\dot{\boldsymbol{\Omega}} = \mathbf{R}^T \dot{\mathbf{w}}_g \quad (85)$$

Inserting Eqs. (66), (71), (78), (82) and (85) into Eq. (65), the inertia force vector is obtained as

$$\begin{aligned} f_I = \int_{l_0} [ & \mathbf{E} \mathbf{H}_2^T \mathbf{R}_r^T A_\rho \dot{\mathbf{H}}_1 + \mathbf{E} \mathbf{H}_2^T A_\rho (\widetilde{\mathbf{w}}_r^e \mathbf{H}_2 + \dot{\mathbf{H}}_2 - \mathbf{H}_2 \dot{\mathbf{E}}_r) \mathbf{E}^T \dot{\mathbf{q}}_g \\ & + \mathbf{E} \mathbf{H}_2^T A_\rho \mathbf{H}_2 \mathbf{E}^T \ddot{\mathbf{q}}_g + \mathbf{E} \mathbf{H}_3^T \bar{\mathbf{R}} (J_\rho \bar{\mathbf{R}}^T \dot{\mathbf{w}}_e + \widetilde{\boldsymbol{\Omega}} J_\rho \boldsymbol{\Omega}) ] d\chi \end{aligned} \quad (86)$$

where  $\bar{\mathbf{R}}$  denotes the local rotation matrix. Assuming the local rotation is small,  $\bar{\mathbf{R}}$  can be approximately expressed as

$$\bar{\mathbf{R}} = \mathbf{R}_r^T \mathbf{R} \approx (\mathbf{I} + \widetilde{\boldsymbol{\theta}}) \quad (87)$$

Finally, from Eqs. (32), (36), (62), (65) and (86), the equation of motion of the element is obtained as

$$f_I(\mathbf{q}_g, \dot{\mathbf{q}}_g, \ddot{\mathbf{q}}_g) + f_G(\mathbf{q}_g) = \mathbf{f} \quad (88)$$

## 5. Numerical algorithms

The nonlinear equations of motion of the discrete system will be solved using the Newton-Raphson method. Because of the strong nonlinearity of the dynamic problem studied in this paper, numerical damping should be introduced to avoid numerical

instability. The HHT method [43, 44] is used to discretize the system in time.

### 5.1. Tangent stiffness matrix and dynamic matrix

To linearize Eq. (88), the following matrices should be obtained

$$\mathbf{M} = \frac{\partial \mathbf{f}_I}{\partial \dot{\mathbf{q}}_g}, \quad \mathbf{C} = \frac{\partial \mathbf{f}_I}{\partial \dot{\mathbf{q}}_g}, \quad \mathbf{K} = \frac{\partial \mathbf{f}_G}{\partial \mathbf{q}_g} + \frac{\partial \mathbf{f}_I}{\partial \mathbf{q}_g} = \mathbf{K}_T + \mathbf{K}_I \quad (89)$$

where  $\mathbf{M}$ ,  $\mathbf{C}$  and  $\mathbf{K}_I$  are the mass, gyroscopic and centrifugal dynamic matrices, respectively.  $\mathbf{K}_T$  is the global tangent stiffness matrix.

From Eqs. (86) and (89), the mass matrix is given by

$$\mathbf{M}_K = \int_{l_0} (\mathbf{E} \mathbf{H}_2^T \mathbf{A}_\rho \mathbf{H}_2 \mathbf{E}^T + \mathbf{E} \mathbf{H}_3^T \bar{\mathbf{R}} \mathbf{J}_\rho \bar{\mathbf{R}}^T \mathbf{H}_3 \mathbf{E}^T) d\chi \quad (90)$$

Further, inserting Eqs. (63), (81) and (86) into Eq. (89), the gyroscopic dynamic matrix is obtained as

$$\begin{aligned} \mathbf{C} = \int_{l_0} & \left[ \mathbf{E} \mathbf{H}_2^T \mathbf{R}_r^T \mathbf{A}_\rho \frac{\partial \dot{\mathbf{H}}_1}{\partial \dot{\mathbf{q}}_g} - \mathbf{E} \mathbf{H}_2^T \mathbf{A}_\rho (\widetilde{\mathbf{H}_2 \mathbf{Q}_1}) \frac{\partial \dot{\mathbf{w}}_r^e}{\partial \dot{\mathbf{q}}_g} + \mathbf{E} \mathbf{H}_2^T \mathbf{A}_\rho \frac{\partial \dot{\mathbf{H}}_2}{\partial \dot{\mathbf{q}}_g} \mathbf{Q}_1 \right. \\ & - \mathbf{E} \mathbf{H}_2^T \mathbf{A}_\rho \mathbf{H}_2 \frac{\partial \dot{\mathbf{E}}_r}{\partial \dot{\mathbf{q}}_g} \mathbf{Q}_1 + \mathbf{E} \mathbf{H}_2^T \mathbf{A}_\rho (\widetilde{\mathbf{w}}_r^e \mathbf{H}_2 + \dot{\mathbf{H}}_2 - \mathbf{H}_2 \dot{\mathbf{E}}_r) \mathbf{E}^T \\ & \left. + \mathbf{E} \mathbf{H}_3^T \bar{\mathbf{R}} \mathbf{J}_\rho \bar{\mathbf{R}}^T \frac{\partial \dot{\mathbf{w}}_e}{\partial \dot{\mathbf{q}}_g} + \mathbf{E} \mathbf{H}_3^T \bar{\mathbf{R}} (\tilde{\mathbf{J}}_\rho - (\widetilde{\mathbf{J}_\rho \boldsymbol{\Omega}})) \bar{\mathbf{R}}^T \frac{\partial \dot{\mathbf{w}}_e}{\partial \dot{\mathbf{q}}_g} \right] d\chi \end{aligned} \quad (91)$$

with  $\mathbf{Q}_1 = \dot{\mathbf{q}}_g^e = \mathbf{E}^T \dot{\mathbf{q}}_g$ ,  $\partial \dot{\mathbf{H}}_1 / \partial \dot{\mathbf{q}}_g$ ,  $\partial \dot{\mathbf{H}}_2 / \partial \dot{\mathbf{q}}_g \mathbf{Q}_1$  and  $\frac{\partial \dot{\mathbf{E}}_r}{\partial \dot{\mathbf{q}}_g} \mathbf{Q}_1$  given in [Appendix C](#).

Using Eq. (55), (81) and (82),  $\partial \dot{\mathbf{w}}_r^e / \partial \dot{\mathbf{q}}_g$ ,  $\partial \dot{\mathbf{w}}_e / \partial \dot{\mathbf{q}}_g$  and  $\partial \ddot{\mathbf{w}}_e / \partial \dot{\mathbf{q}}_g$  can be obtained as

$$\frac{\partial \dot{\mathbf{w}}_r^e}{\partial \dot{\mathbf{q}}_g} = \frac{\partial \mathbf{w}_r^e}{\partial \mathbf{q}_g} = \mathbf{G}_1^T \mathbf{E}^T \quad (92)$$

$$\frac{\partial \dot{\mathbf{w}}_e}{\partial \dot{\mathbf{q}}_g} = \mathbf{H}_3 \mathbf{E}^T \quad (93)$$

$$\begin{aligned} \frac{\partial \ddot{\mathbf{w}}_e}{\partial \dot{\mathbf{q}}_g} = & (\widetilde{\dot{\mathbf{w}}_r^e} \mathbf{H}_3 + \dot{\mathbf{H}}_3 - \mathbf{H}_3 \dot{\mathbf{E}}_r) \mathbf{E}^T - (\widetilde{\mathbf{H}_3 \mathbf{Q}_1}) \frac{\partial \dot{\mathbf{w}}_r^e}{\partial \dot{\mathbf{q}}_g} + \frac{\partial \dot{\mathbf{H}}_3}{\partial \dot{\mathbf{q}}_g} \mathbf{Q}_1 - \mathbf{H}_3 \frac{\partial \dot{\mathbf{E}}_r}{\partial \dot{\mathbf{q}}_g} \mathbf{Q}_1 \\ & - \widetilde{\mathbf{H}_4} \frac{\partial \dot{\mathbf{w}}_r^e}{\partial \dot{\mathbf{q}}_g} + \frac{\partial \dot{\mathbf{H}}_4}{\partial \dot{\mathbf{q}}_g} \end{aligned} \quad (94)$$

with  $\partial \dot{\mathbf{H}}_3 / \partial \dot{\mathbf{q}}_g \mathbf{Q}_1$ ,  $\partial \dot{\mathbf{E}}_r / \partial \dot{\mathbf{q}}_g \mathbf{Q}_1$  and  $\partial \dot{\mathbf{H}}_4 / \partial \dot{\mathbf{q}}_g$  given in [Appendix C](#).

From Eqs. (61), (62) and (89), one obtains

$$\mathbf{K}_T = \frac{\partial \mathbf{f}_G}{\partial \mathbf{q}_g} = \mathbf{B}_1^T \mathbf{K}_L \mathbf{B}_1 + f_{L1} \widehat{\mathbf{U}}^T + \mathbf{E} \widehat{\mathbf{P}}_1^T \mathbf{Q}_2 + \mathbf{E} \widehat{\mathbf{E}}_r \mathbf{Q}_3 \quad (95)$$

with  $\widehat{[\ ]} = \partial[\ ] / \partial \mathbf{q}_g$ ,  $\mathbf{Q}_2 = [f_{L2} \ f_{L3} \ f_{L4} \ f_{L5} \ f_{L6} \ f_{L7}]^T$  and  $\mathbf{Q}_3 = \mathbf{P}_1^T \mathbf{Q}_2$ .

$\widehat{\mathbf{P}}_1^T \mathbf{Q}_2$  and  $\widehat{\mathbf{E}}_r \mathbf{Q}_3$  are given in [Appendix C](#). Using Eqs. (45) and (A.3),  $\widehat{\mathbf{U}}^T$  can be obtained as

$$\widehat{\mathbf{U}}^T = \frac{\partial \bar{\mathbf{U}}^T}{\partial \mathbf{q}_g} = \frac{1}{l_c} \begin{bmatrix} -\mathbf{I} \\ \mathbf{0} \\ \mathbf{I} \\ \mathbf{0} \end{bmatrix} [\mathbf{I} - \mathbf{r}_1 \otimes \mathbf{r}_1] [-\mathbf{I} \ \mathbf{0} \ \mathbf{I} \ \mathbf{0}] \quad (96)$$

From Eqs. (86) and (89),  $\mathbf{K}_I$  can be expanded as

$$\begin{aligned}
K_1 = \frac{\partial f_l}{\partial \mathbf{q}_g} = \int_{l_0} \big[ & (\mathbf{E}\widehat{\mathbf{E}}_r \mathbf{Q}_4 + \mathbf{E}\widehat{\mathbf{H}}_2^T \mathbf{Q}_5 + \mathbf{E}\mathbf{H}_2^T (\mathbf{R}_r^T \widetilde{\mathbf{A}_\rho \dot{\mathbf{H}}_1}) \widehat{\mathbf{w}}_r^e + \mathbf{E}\mathbf{H}_2^T \mathbf{R}_r^T \mathbf{A}_\rho \widehat{\mathbf{H}}_1) \\
& + \mathbf{E}\mathbf{H}_2^T \mathbf{A}_\rho (\widehat{\mathbf{w}}_r^e \widehat{\mathbf{H}}_2 \mathbf{Q}_1 - (\widetilde{\mathbf{H}_2 \mathbf{Q}_1}) \widehat{\mathbf{w}}_r^e + \widehat{\mathbf{H}}_2 \mathbf{Q}_1 + \widehat{\mathbf{H}}_2 \mathbf{Q}_6 \\
& - \mathbf{H}_2 \widehat{\mathbf{E}}_r \mathbf{Q}_1) - \mathbf{E}\mathbf{H}_2^T \mathbf{A}_\rho (\widehat{\mathbf{w}}_r^e \mathbf{H}_2 + \dot{\mathbf{H}}_2 - \mathbf{H}_2 \dot{\mathbf{E}}_r) \widehat{\mathbf{E}}_r \mathbf{Q}_1 \\
& + \mathbf{E}\mathbf{H}_2^T \mathbf{A}_\rho \widehat{\mathbf{H}}_2 \mathbf{Q}_7 - \mathbf{E}\mathbf{H}_2^T \mathbf{A}_\rho \mathbf{H}_2 \widehat{\mathbf{E}}_r \mathbf{Q}_7 \big] \\
& + \big[ \mathbf{E}\widehat{\mathbf{E}}_r \mathbf{Q}_8 + \mathbf{E}\widehat{\mathbf{H}}_3^T \mathbf{Q}_9 - \mathbf{E}\mathbf{H}_3^T (\mathbf{J}_\rho \bar{\mathbf{R}}^T \widetilde{\mathbf{w}_e} + \widetilde{\tilde{\mathbf{N}} \mathbf{J}_\rho \Omega}) \widehat{\boldsymbol{\theta}} \\
& + \mathbf{E}\mathbf{H}_3^T \bar{\mathbf{R}} \mathbf{J}_\rho \widehat{\mathbf{w}}_e \widehat{\boldsymbol{\theta}} + \mathbf{E}\mathbf{H}_3^T \bar{\mathbf{R}} \mathbf{J}_\rho \bar{\mathbf{R}}^T \widehat{\mathbf{w}}_e \\
& + \mathbf{E}\mathbf{H}_3^T \bar{\mathbf{R}} (\widetilde{\tilde{\mathbf{N}} \mathbf{J}_\rho} - (\widetilde{\mathbf{J}_\rho \Omega}) \widehat{\boldsymbol{\Omega}} \big] d\chi
\end{aligned} \tag{97}$$

with

$$\begin{aligned}
\mathbf{Q}_4 &= \mathbf{H}_2^T \mathbf{R}_r^T \mathbf{A}_\rho \ddot{\mathbf{u}}, \quad \mathbf{Q}_5 = \mathbf{R}_r^T \mathbf{A}_\rho \ddot{\mathbf{u}}, \quad \mathbf{Q}_6 = \dot{\mathbf{E}}^T \dot{\mathbf{q}}_g, \quad \mathbf{Q}_7 = \mathbf{E}^T \ddot{\mathbf{q}}_g \\
\mathbf{Q}_8 &= \mathbf{H}_3^T \bar{\mathbf{R}} (\mathbf{J}_\rho \bar{\mathbf{R}}^T \widetilde{\mathbf{w}_e} + \widetilde{\tilde{\mathbf{N}} \mathbf{J}_\rho \Omega}), \quad \mathbf{Q}_9 = \bar{\mathbf{R}} (\mathbf{J}_\rho \bar{\mathbf{R}}^T \widetilde{\mathbf{w}_e} + \widetilde{\tilde{\mathbf{N}} \mathbf{J}_\rho \Omega}).
\end{aligned} \tag{98}$$

$\widehat{\mathbf{w}}_r^e$  is obtained from Eq. (92).  $\widehat{\mathbf{H}}_2^T \mathbf{Q}_5$ ,  $\mathbf{R}_r^T \widehat{\mathbf{H}}_1$ ,  $\widehat{\mathbf{H}}_2 \mathbf{Q}_k (k = 1, 6, 7)$ ,  $\widehat{\mathbf{H}}_2 \mathbf{Q}_1$ ,  $\widehat{\mathbf{E}}_r \mathbf{Q}_1$ ,  $\widehat{\mathbf{H}}_3^T \mathbf{Q}_9$ ,  $\widehat{\boldsymbol{\theta}}$ ,  $\widehat{\mathbf{w}}_e$  and  $\widehat{\boldsymbol{\Omega}}$  are given in [Appendix C](#).

## 5.2. Time stepping algorithm

Considering the finite rotation is non-additive and non-commutative, the iterative forms of node displacements can be expressed as [\[35, 41, 49\]](#)

$$\mathbf{u}_{(n+1)} = \mathbf{u}_{(n)} + \Delta t \dot{\mathbf{u}}_{(n)} + (\Delta t)^2 \left[ \left( \frac{1}{2} - \beta \right) \ddot{\mathbf{u}}_{(n)} + \beta \ddot{\mathbf{u}}_{(n+1)} \right] \tag{99}$$

$$\dot{\mathbf{u}}_{(n+1)} = \dot{\mathbf{u}}_{(n)} + \Delta t [(1 - \gamma) \ddot{\mathbf{u}}_{(n)} + \gamma \ddot{\mathbf{u}}_{(n+1)}] \tag{100}$$



$$\boldsymbol{\theta}_{(n+1)}^g = \Delta t \dot{\mathbf{w}}_{(n)} + (\Delta t)^2 \left[ \left( \frac{1}{2} - \beta \right) \ddot{\mathbf{w}}_{(n)} + \beta \ddot{\mathbf{w}}_{(n+1)} \right] \quad (101)$$

$$\dot{\mathbf{w}}_{(n+1)} = \boldsymbol{\Lambda}_{(n+1)}^g [\dot{\mathbf{w}}_{(n)} + \Delta t (1 - \gamma) \ddot{\mathbf{w}}_{(n)}] + \Delta t \gamma \ddot{\mathbf{w}}_{(n+1)} \quad (102)$$

$$\boldsymbol{\Lambda}_{(n+1)}^g = \exp \left( \widetilde{\boldsymbol{\theta}_{(n+1)}^g} \right) = \mathbf{R}_{(n+1)} \mathbf{R}_{(n)}^T \quad (103)$$

where  $\Delta t$  denotes the time step and the subscript  $(n + 1)$  denotes the  $(n + 1)$ th step. The values of  $\beta$  and  $\gamma$  can be obtained as in [43]. The linearizations of the velocity and acceleration are given by

$$\Delta \dot{\mathbf{u}}_{(n+1)} = \frac{\gamma}{\beta \Delta t} (\mathbf{u}_{(n+1)} - \mathbf{u}_{(n)}) \quad (104)$$

$$\Delta \ddot{\mathbf{u}}_{(n+1)} = \frac{1}{\beta (\Delta t)^2} (\mathbf{u}_{(n+1)} - \mathbf{u}_{(n)}) \quad (105)$$

$$\Delta \dot{\mathbf{w}}_{(n+1)} = \frac{\gamma}{\beta \Delta t} \mathbf{T}^{-T} \left( \boldsymbol{\theta}_{(n+1)}^g \right) \Delta \mathbf{w}_{(n+1)} \quad (106)$$

$$\Delta \ddot{\mathbf{w}}_{(n+1)} = \frac{1}{\beta (\Delta t)^2} \mathbf{T}^{-T} \left( \boldsymbol{\theta}_{(n+1)}^g \right) \Delta \mathbf{w}_{(n+1)} \quad (107)$$

where the operator  $\mathbf{T}^{-1}(\cdot)$  can be obtained using Eq. (40)

$$\mathbf{T}^{-1}(\boldsymbol{\theta}) = \frac{\theta}{2} \cot \left( \frac{\theta}{2} \right) \mathbf{I} - \frac{1}{2} \tilde{\boldsymbol{\theta}} + \left( 1 - \frac{\theta}{2} \cot \left( \frac{\theta}{2} \right) \right) \boldsymbol{\theta} \boldsymbol{\theta}^T \quad (108)$$

with the relationship [50]

$$\mathbf{T}^{-T}(\boldsymbol{\theta}) = \exp(\tilde{\boldsymbol{\theta}}) \mathbf{T}^{-1}(\boldsymbol{\theta}) \quad (109)$$

According to the relations (99)-(103), the update procedures of the displacements, velocities and accelerations at the  $k$ th iteration of step  $(n+1)$  are performed as follows [51]

$$\mathbf{u}_{(n+1)}^{(k)} = \mathbf{u}_{(n+1)}^{(k-1)} + \Delta \mathbf{u}_{(n+1)}^{(k)} \quad (110)$$

$$\dot{\mathbf{u}}_{(n+1)}^{(k)} = \frac{\gamma}{\beta \Delta t} \left( \mathbf{u}_{(n+1)}^{(k)} - \mathbf{u}_{(n)} \right) + \frac{\beta - \gamma}{\beta} \dot{\mathbf{u}}_{(n)} + \frac{2\beta - \gamma}{2\beta} \Delta t \ddot{\mathbf{u}}_{(n)} \quad (111)$$

$$\ddot{\mathbf{u}}_{(n+1)}^{(k)} = \frac{1}{\beta (\Delta t)^2} \left( \mathbf{u}_{(n+1)}^{(k)} - \mathbf{u}_{(n)} \right) - \frac{1}{\beta \Delta t} \dot{\mathbf{u}}_{(n)} + \frac{2\beta - 1}{2\beta} \ddot{\mathbf{u}}_{(n)} \quad (112)$$

$$\exp \left( \widetilde{\boldsymbol{\theta}_{(n+1)}^{g,(k)}} \right) = \exp \left( \widetilde{\Delta \mathbf{w}_{(n+1)}^{(k)}} \right) \exp \left( \widetilde{\boldsymbol{\theta}_{(n+1)}^{g,(k-1)}} \right) \quad (110)$$

$$\mathbf{R}_{i,(n+1)}^{g,(k)} = \exp \left( \widetilde{\boldsymbol{\theta}_{(n+1)}^{g,(k)}} \right) \mathbf{R}_{i,(n)}^g, \quad i = 1, 2. \quad (113)$$

$$\dot{\mathbf{w}}_{(n+1)}^{(k)} = \boldsymbol{\Lambda}_{(n+1)}^{g,(k)} \left( \frac{\gamma}{\beta \Delta t} \boldsymbol{\theta}_{(n+1)}^{g,(k)} + \frac{\beta - \gamma}{\beta} \dot{\mathbf{w}}_{(n)} + \frac{2\beta - \gamma}{2\beta} \Delta t \ddot{\mathbf{w}}_{(n)} \right) \quad (114)$$

$$\ddot{\mathbf{w}}_{(n+1)}^{(k)} = \boldsymbol{\Lambda}_{(n+1)}^{g,(k)} \left( \frac{1}{\beta (\Delta t)^2} \boldsymbol{\theta}_{(n+1)}^{g,(k)} - \frac{1}{\beta \Delta t} \dot{\mathbf{w}}_{(n)} + \frac{2\beta - 1}{2\beta} \ddot{\mathbf{w}}_{(n)} \right) \quad (115)$$

where  $\mathbf{R}_{i,(n)}^g (i = 1, 2)$  denotes the converged solution of  $\mathbf{R}_i^g$  at  $n$ th step.

In the HHT method, the nonlinear equation of motion (88) is rewritten as [44, 49]

$$\mathbf{f}_{I,(n+1)} + (1 + \alpha) (\mathbf{f}_{G,(n+1)} - \mathbf{f}_{(n+1)}) - \alpha (\mathbf{f}_{G,(n)} - \mathbf{f}_{(n)}) = \mathbf{0} \quad (116)$$

where  $\alpha$  is a parameter giving a numerical damping.

Finally, from Eqs. (89) and (110)-(116), the following equation should be solved to

obtain the incremental displacement at the  $k$ th iteration of step  $(n+1)$ , i.e.

$$\mathbf{K}_{\text{Total},(n+1)}^{(k)} \Delta \mathbf{q}_{(n+1)}^{(k)} = \mathbf{f}_{\text{Total},(n+1)}^{(k)} \quad (117)$$

with

$$\Delta \mathbf{q}_{(n+1)}^{(k)} = \left[ \left( \Delta \mathbf{u}_{1,(n+1)}^{(k)} \right)^T \quad \left( \Delta \mathbf{w}_{1,(n+1)}^{(k)} \right)^T \quad \left( \Delta \mathbf{u}_{2,(n+1)}^{(k)} \right)^T \quad \left( \Delta \mathbf{w}_{2,(n+1)}^{(k)} \right)^T \right]^T \quad (118)$$

$$\mathbf{f}_{\text{Total},(n+1)}^{(k)} = (1 + \alpha) \left( \mathbf{f}_{(n+1)}^{(k)} - \mathbf{f}_{G,(n+1)}^{(k)} \right) + \alpha \left( \mathbf{f}_{G,(n+1)}^{(k-1)} - \mathbf{f}_{(n+1)}^{(k-1)} \right) - \mathbf{f}_{I,(n+1)}^{(k)} \quad (119)$$

and the iterative tangent matrix

$$\begin{aligned} \mathbf{K}_{\text{Total},(n+1)}^{(k)} &= (1 + \alpha) \mathbf{K}_T + \mathbf{K}_{I,(n+1)}^{(k)} + \frac{\gamma}{\beta \Delta t} \mathbf{C}_{(n+1)}^{(k)} \mathbf{B}_{(n+1)}^{(k)} \\ &\quad + \frac{1}{\beta (\Delta t)^2} \mathbf{M}_{(n+1)}^{(k)} \mathbf{B}_{(n+1)}^{(k)} \end{aligned} \quad (120)$$

with

$$\mathbf{B}_{(n+1)}^{(k)} = \begin{bmatrix} \mathbf{I} & \mathbf{0} & \mathbf{0} & \mathbf{0} \\ \mathbf{0} & \mathbf{T}^{-T} \left( \boldsymbol{\theta}_{1,(n+1)}^{g,(k)} \right) & \mathbf{0} & \mathbf{0} \\ \mathbf{0} & \mathbf{0} & \mathbf{I} & \mathbf{0} \\ \mathbf{0} & \mathbf{0} & \mathbf{0} & \mathbf{T}^{-T} \left( \boldsymbol{\theta}_{2,(n+1)}^{g,(k)} \right) \end{bmatrix} \quad (121)$$

## 6. Numerical examples

Four examples are given in this section. The first example, introduced by Steinbrecher et al. [15], is used to verify the validity of the proposed dynamic formulations in dealing with a 2D sliding beam problem. The second example extends

the 2D cantilever beam model introduced by Le et al. [52] to the 3D case. The beam can rotate about the clamped end with a given angular velocity. The third example is used to study the dynamics of a 3D sliding beam. In the last example, a beam manipulated by a revolute-prismatic joint can not only undergo large overall motion but can also slide through the joint. It should be noted that the nodal displacement of the simulation curve is defined by Eq. (11) in the following examples.

In the process of computation, the global elastic force vector  $\mathbf{f}_G$  and the global tangent stiffness matrix  $\mathbf{K}_T$  can be exactly evaluated by Eqs. (62) and (95). To obtain the inertia force vector  $\mathbf{f}_I$ , mass matrix  $\mathbf{M}$ , gyroscopic matrix  $\mathbf{C}$  and centrifugal matrix  $\mathbf{K}_I$ , three Gauss points are used to integrate Eqs. (86), (90), (91) and (97). The time step is set to  $\Delta t = 1 \times 10^{-4}$ s. The following convergence criterion is adopted: the norm of the residual virtual work must be less than the prescribed tolerance  $10^{-5}$ .

## 6.1. Example 1

As shown in Fig. 4(a), a cantilever beam of initial length  $L(0) = 5$ m is subjected to a uniform body force  $P_y = 1$ kN/m<sup>3</sup> in the negative y-axis direction and is in static equilibrium at  $t = 0$ . The width and the height of the cross-section are  $b = 1$ m and  $h = 0.2$ m, respectively. The elastic modulus and the density of the beam are  $E = 10$ MPa and  $\rho = 10^3$ kg/m<sup>3</sup>, respectively. When  $t > 0$ , the beam begins to retract into the channel, and the retraction acceleration is depicted in Fig. 4(b).

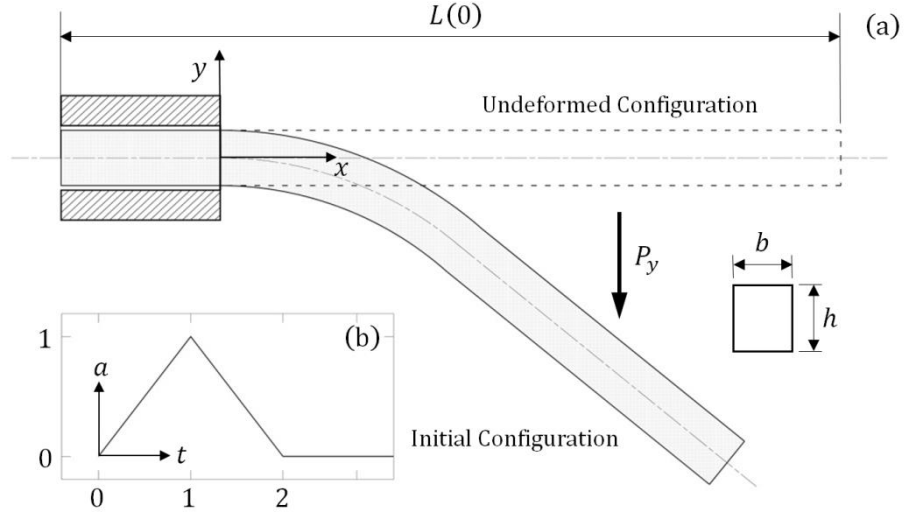


**Fig. 4** 2D sliding beam dynamic problem: (a) sliding beam model; (b) retraction acceleration curve

To obtain the reference solution, 20 elements are used to discretize the beam. The horizontal and vertical displacement histories of the free endpoint of the cantilever beam are depicted in Figs. 5 and 6, respectively. It can be observed that the simulation results with only 8 elements have sufficient computational accuracy. Making a comparison between these results and those obtained by Steinbrecher et al. [15] using the commercial software ABAQUS, there are some differences but they have the same trend, as shown in Fig. 6. These differences are partly because Steinbrecher et al. have taken the vibration of the beam in the channel into account. Additionally, when calculating the static equilibrium configuration of the beam, they assumed that the beam can slide out of the channel by a small amount. To investigate the effect of this small amount on the dynamic response of the beam, the initial length is modified to  $L(0) = 5.09$  m. The

corresponding result obtained by the presented method is almost identical to that of Steinbrecher et al., as shown in Fig. 6.

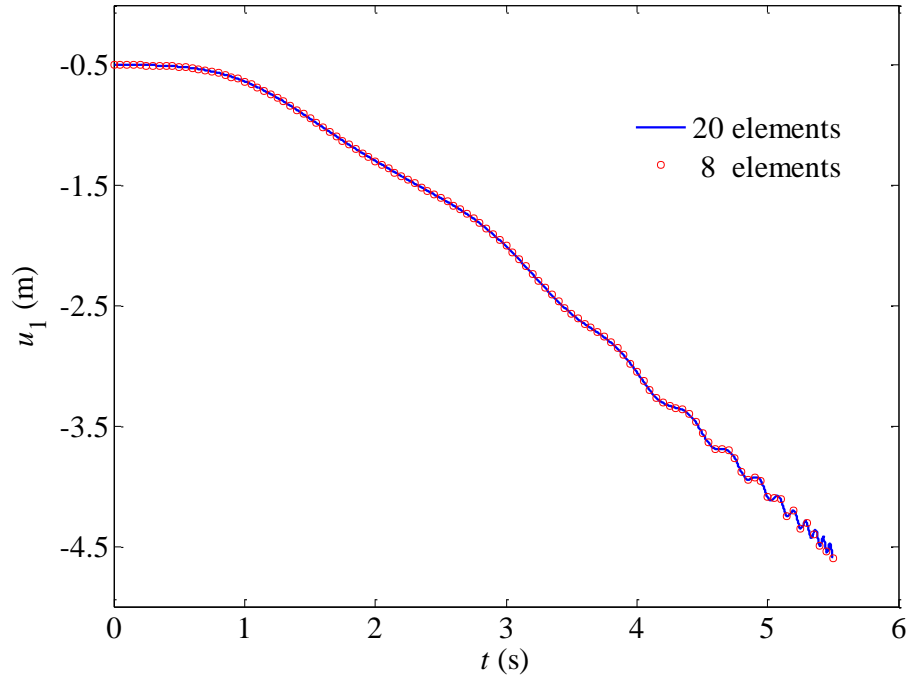


**Fig. 5** 2D sliding beam: horizontal displacement history

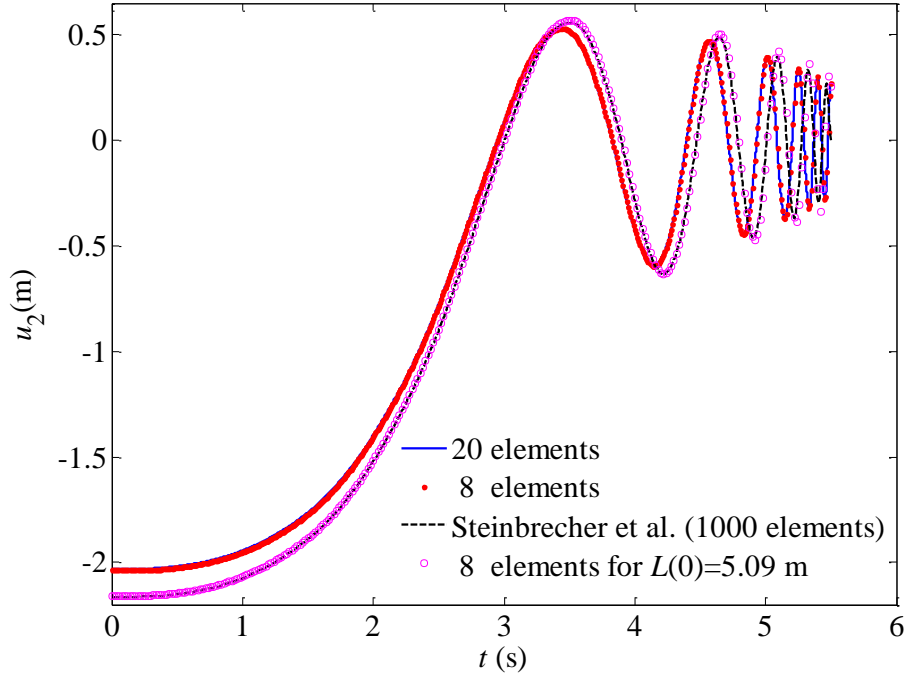


**Fig. 6** 2D sliding beam: vertical displacement history

## 6.2. Example 2

As shown in Fig. 7(a), a cantilever of length  $L = 10\text{m}$  with rectangular cross-section is subjected to a concentrated force  $F_y = F_0 \sin(\omega_1 t)$  with  $F_0 = 10\text{MN}$ , and  $\omega_1 = 50\text{rad/s}$  at the free end. The cross-section width and height are  $b = 0.25\text{m}$  and  $h = 0.5\text{m}$ , respectively. The elastic modulus and the density of the beam are  $E = 210\text{GPa}$  and  $\rho = 7850\text{kg/m}^3$ , respectively. The beam can be rotated with a prescribed angular velocity about the  $y$ -axis with the clamped end as the center. The time history curve of the angular velocity  $\omega_2$  is depicted in Fig. 7(b).  $\omega_f$  is a given fixed value. When  $\omega_f = 0$ , this example is reduced to the case given by Le et al. [52].

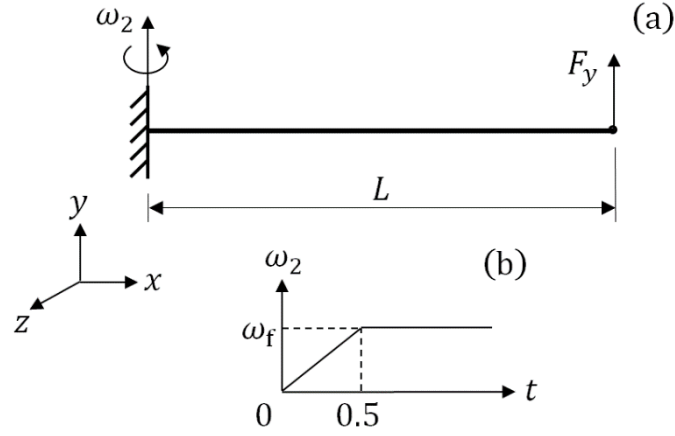


**Fig. 7** 3D rotating beam dynamic problem: (a) rotating beam model; (b) time history of  $\omega_2$

In this example, 10 elements are used to obtain a converged solution. The parameter of the HHT method is set as  $\alpha = -0.05$ . Figs. 8, 9 and 10 show the time history curves of the displacement of the free end in three directions. When  $\omega_f$  takes different values the curves are all depicted in the same figure for comparison. As shown in Fig. 9, it can be found that the vibration frequency of the free end will increase with an increase in  $\omega_2$ . This is because increasing  $\omega_2$  will increase the centrifugal force on the beam, making it more rigid. In particular, when  $\omega_2 = 0$ , these curves are almost identical to the results obtained by Le et al. [52]. This is because the 2D dynamic formulation proposed by Le et al. is a special case of the formulation in this paper.



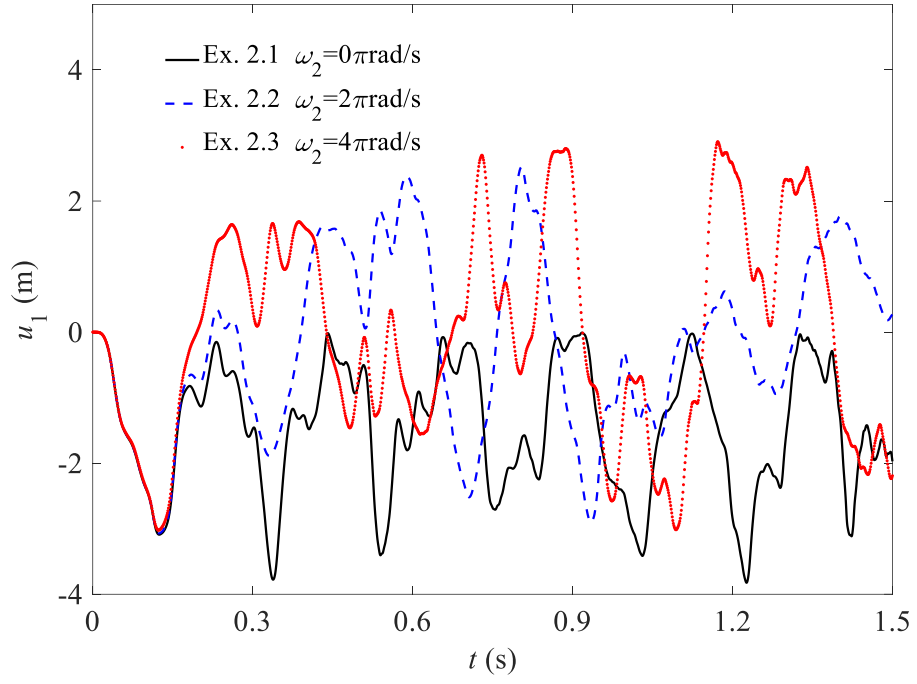


**Fig. 8** 3D rotating beam: time history of the displacement  $u_1$  of the free end

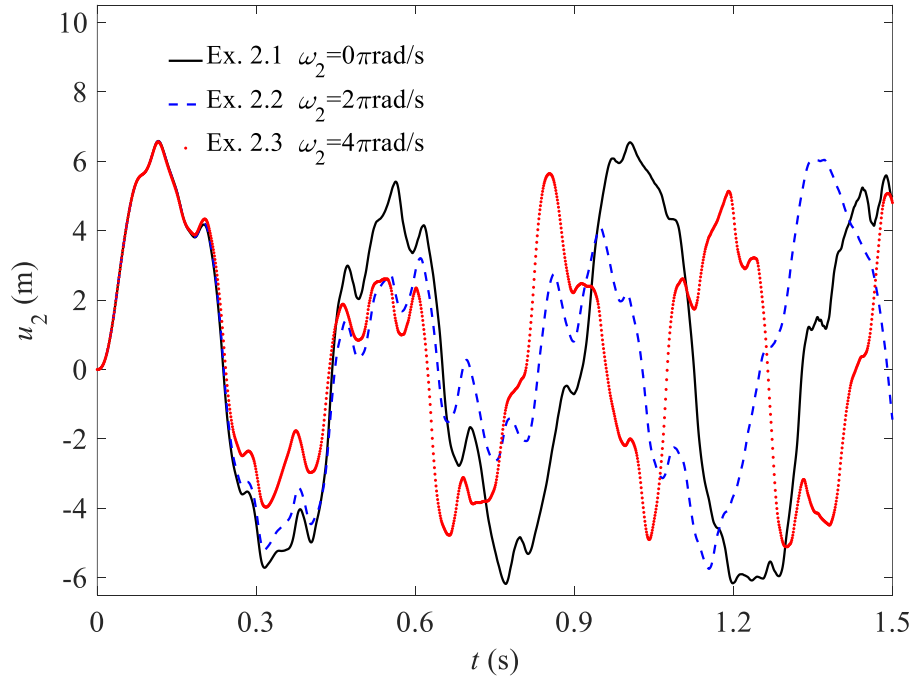


**Fig. 9** 3D rotating beam: time history of the displacement  $u_2$  of the free end

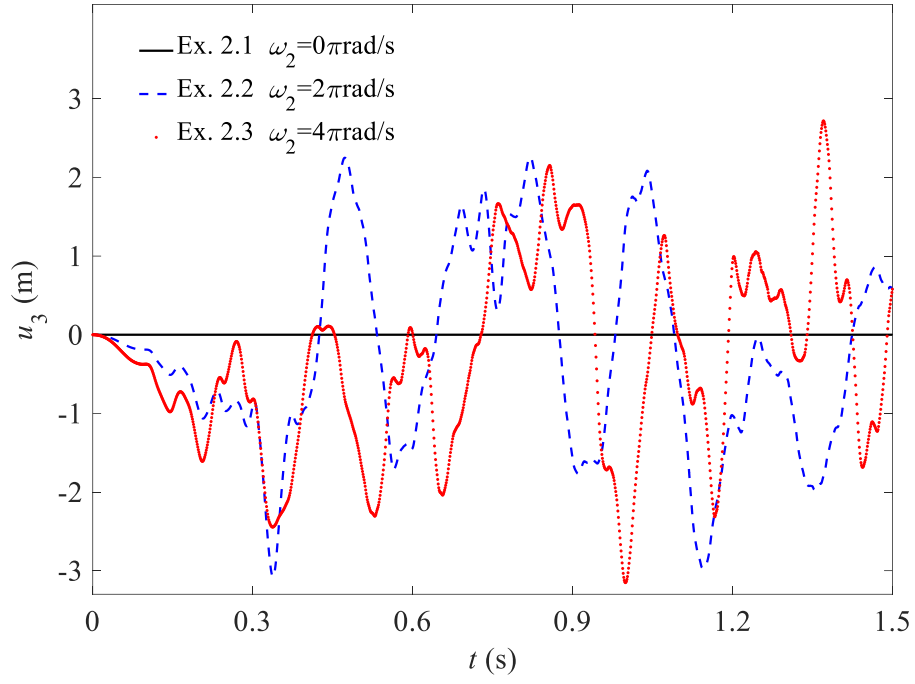


**Fig. 10** 3D rotating beam: time history of the displacement  $u_3$  of the free end

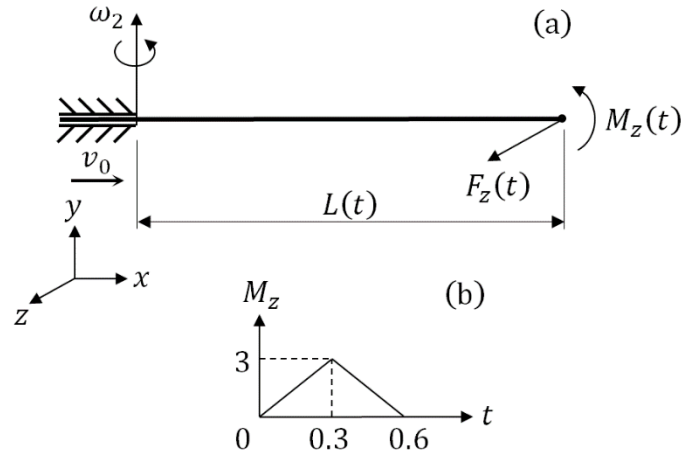


**Fig. 11** 3D sliding beam dynamic problem: (a) sliding beam model; (b) time history of

$$M_z(t)$$

### 6.3. Example 3

As shown in Figs. 11(a) and (b), a cantilever of length  $L = 10\text{m}$  with rectangular

cross-section is subjected to a concentrated force  $F_z(t) = 6\sin(\omega_1 t)$  and a bending moment  $M_z(t)$  at the free end. The cross-section width and the height are  $b = 0.3\text{m}$  and  $h = 0.25\text{m}$ , respectively. The elastic modulus, the Poisson's ratio and the density of the beam are  $E = 210\text{GPa}$ ,  $\nu = 0.3$  and  $\rho = 7850\text{kg/m}^3$ , respectively. The beam can slide through the channel at constant velocity  $v_0$ . When  $v_0 = 0$ , this example reduces to the example given by Le et al. [41].

In this example, 12 elements are used to obtain a converged solution. The parameter of the HHT method is set as  $\alpha = -0.01$ . Figs. 12, 13 and 14 show the time history curves of the displacement of the free end in three directions for different  $v_0$ . When the beam is deployed through the channel, the vibration frequency will decrease. Otherwise, the vibration frequency will increase. Compared with the case for  $v_0 = 0$ , the amplitude of the beam will increase when the beam is deployed or retrieved through the channel. This may be because the sudden increase in axial kinetic energy is converted into elastic potential energy. When  $v_0 = 0$ , these curves are almost identical to those obtained by Le et al. [41]. This is because the 3D dynamic formulation proposed by Le et al. is a special case of the formulation in this paper.

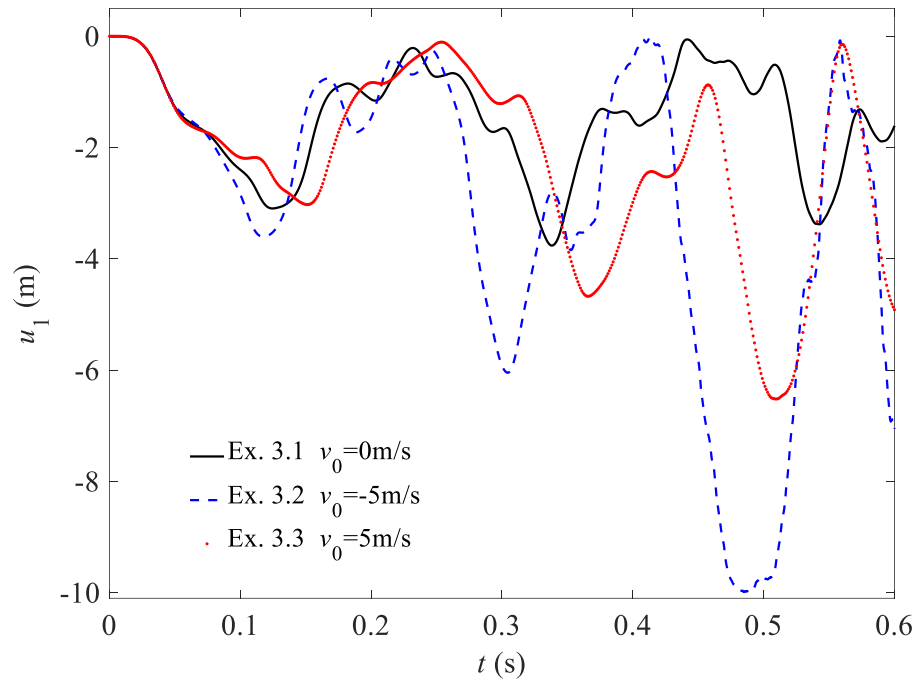


**Fig. 12** 3D sliding beam: time history of the displacement  $u_1$  of the free end

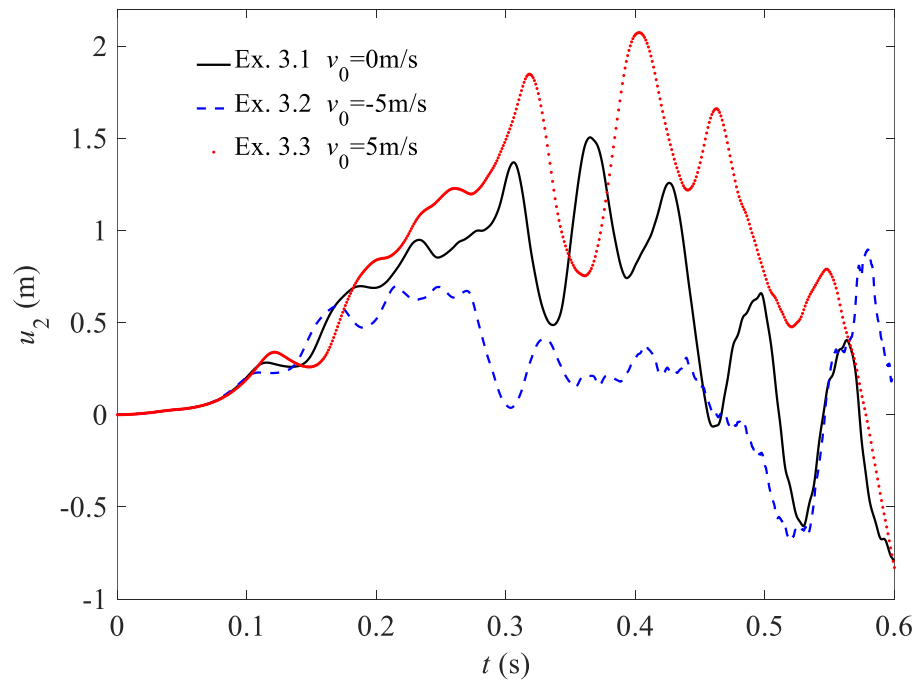


**Fig. 13** 3D sliding beam: time history of the displacement  $u_2$  of the free end

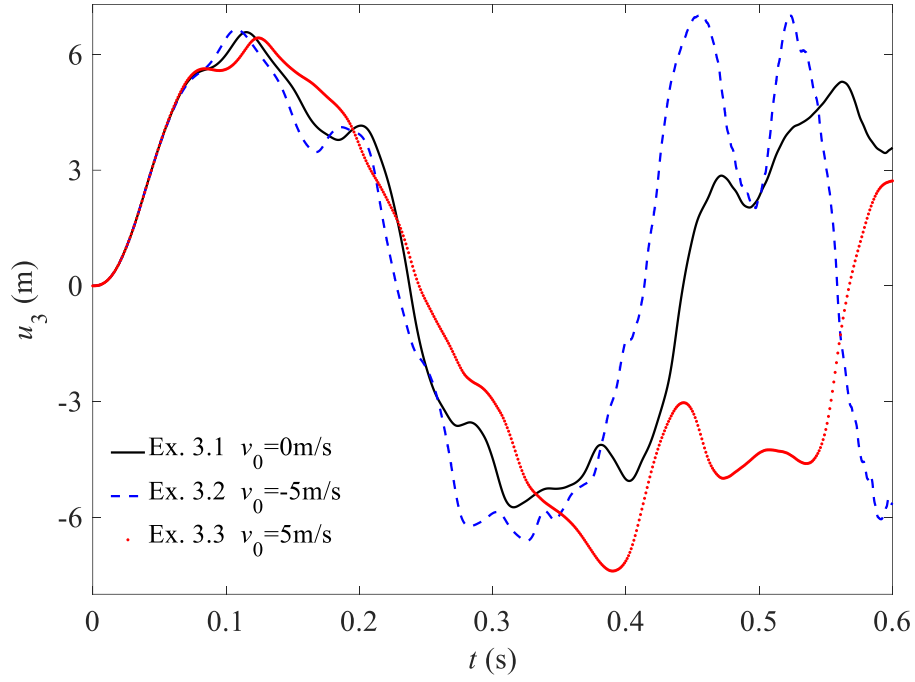


**Fig. 14** 3D sliding beam: time history of the displacement  $u_3$  of the free end

#### 6.4. Example 4

The geometric model, the material properties and the external load of this example are the same as those of example 3. The beam manipulated by the revolute-prismatic joint can undergo large overall motion and slide through the joint. The length of the beam outside the joint channel is  $L = 10 + 5\sin(2\pi t)$ . The prescribed angular velocity of the beam about the  $y$ -axis is the same as that given by example 2.

The geometric nonlinearity of this example is so strong that 100 elements are required to obtain a converged solution. The time history curves of the displacement of the free end in three directions are depicted in Figs. 15, 16 and 17. The parameter of the HHT method is set as  $\alpha = -0.05$ . The vibration frequency increases with increasing  $\omega_2$ .

The phenomenon may be caused by the centrifugal force. In particular, when  $\omega_2 = 4\pi$  rad/s and near the time  $t = 0.4$ s, the displacements of the free end are very large as shown in Figs. 15 and 17. The phenomenon indicates that parametric resonance occurs.

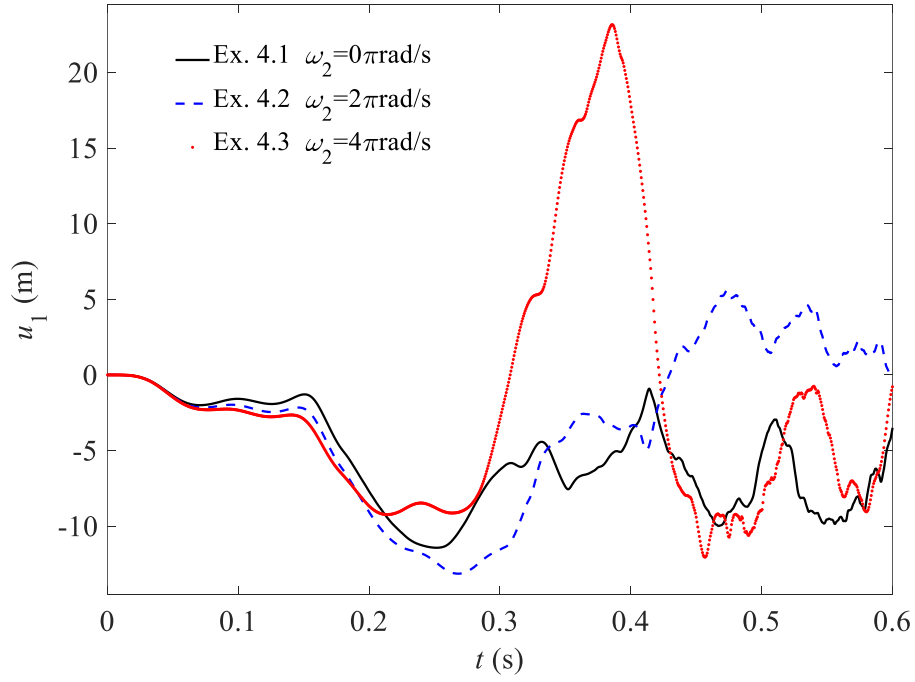


**Fig. 15** 3D rotating-sliding beam: time history of the displacement  $u_1$  of the free end

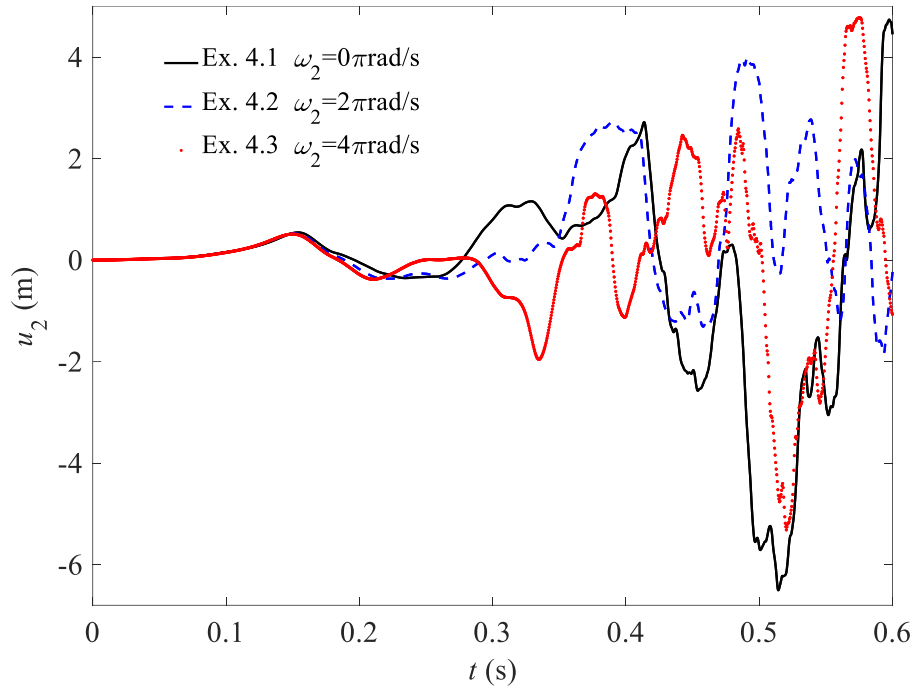


**Fig. 16** 3D rotating-sliding beam: time history of the displacement  $u_2$  of the free end

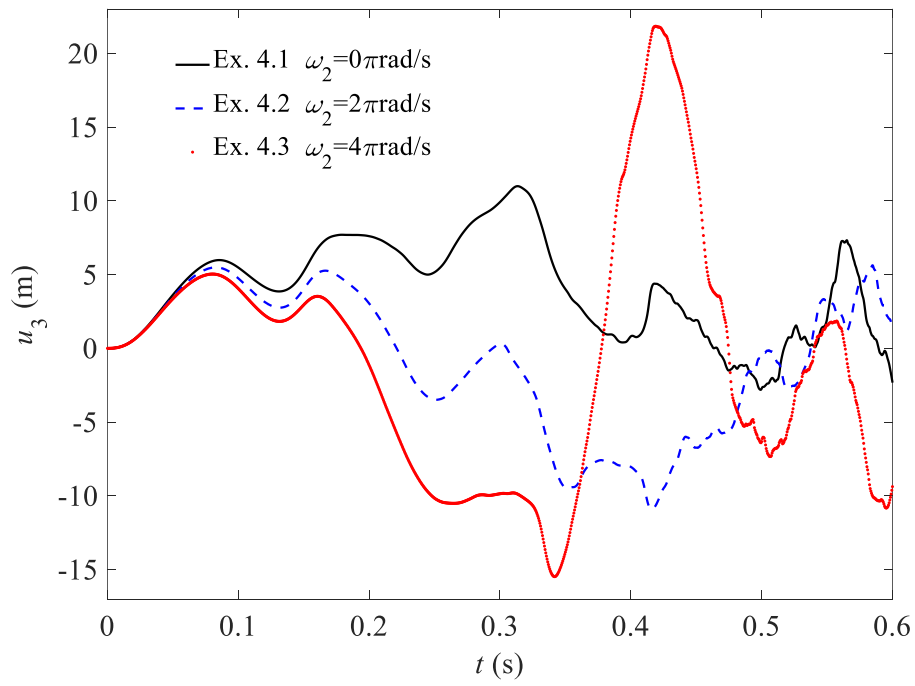


**Fig. 17** 3D rotating-sliding beam: time history of the displacement  $u_3$  of the free end

## 7. Conclusions

Nonlinear dynamic analysis of a 3D sliding beam which can undergo large overall motion has been performed based on the corotational method. To describe the spatial configuration of flexible beams accurately, the rotational vectors were used to parameterize the rotation matrices. The variable-domain IEE elements were used to discretize the time-varying system in space. The extension of Hamilton's principle was used to derive the nonlinear equations of motion which can consider the effects of shear deformation and rotary inertia. The numerical simulations and comparisons of the numerical examples have demonstrated the validity, accuracy and versatility of the dynamic formulae of this paper.

Some dynamic behaviors of the system have been shown by the results. The sliding and the overall motion of the flexible beam have great influence on the amplitude and frequency of the beam. In example 4, with the increase of the rotational angular velocity, the parametric resonance occurs. It should be pointed out that the introduction of the corotational frame makes the expression of the inertia force vector very complicated. To linearize the inertia force vector, the gyroscopic and centrifugal dynamic matrices should be evaluated. These two matrices are more complicated, as shown in Eqs. (91) and (97). These evaluations will lead to a huge increase of computation time for every iteration step. However, if we keep only the mass matrix for iteration based on Newton-Raphson method, the converged solution can be usually obtained [53]. Several examples are used to test the



effects of the gyroscopic matrix  $\mathbf{C}$  and the centrifugal matrix  $\mathbf{K}_I$ . They have no effect on the simulation results but do have an effect on the number of iterations. Compared with  $\mathbf{K}_I$ ,  $\mathbf{C}$  has more potential to reduce the number of iterations. Therefore, it is proposed to ignore the term  $\mathbf{K}_I$  when solving the equation of motion using Newton-Raphson method. This is consistent with the views of Le et al. [41, 49]. At the same time, it should be pointed out that the examples, convergence criteria and the HHT parameter have an influence on the number of iterations which should be studied further.

## Acknowledgments

The authors wish to acknowledge financial support from the National Natural Science Foundation of China (11672060), and the Cardiff University School of Engineering.

## Appendix A

The following relationship will be used in this section, i.e.

$$\mathbf{r}_i^T \delta \mathbf{r}_j = -\mathbf{r}_j^T \delta \mathbf{r}_i, \quad i, j = 1, 2, 3. \quad (\text{A.1})$$

$$\|\mathbf{r}_1 \times \mathbf{p}\| = \mathbf{r}_2^T \mathbf{p} \quad (\text{A.2})$$

By taking the variation of Eqs. (16) and (17), one obtains

$$\delta \mathbf{r}_1 = \frac{1}{l_c} [\mathbf{I} - \mathbf{r}_1 \otimes \mathbf{r}_1] \left( [-\mathbf{I} \quad \mathbf{0} \quad \mathbf{I} \quad \mathbf{0}] \delta \mathbf{q}_g + \frac{v_0 \mathbf{r}_1^0 + L \dot{\mathbf{r}}_1^0}{n} \delta t \right) \quad (\text{A.3})$$

$$\delta \mathbf{p}_k = -\widetilde{\mathbf{p}}_k \delta \mathbf{w}_k^g + \mathbf{R}_k^g \dot{\mathbf{r}}_2^0 \delta t, \quad k = 1, 2. \quad (\text{A.4})$$

Eq. (A.4) can be expressed in a simple form

$$\begin{aligned} \delta \mathbf{p}_1 &= -\widetilde{\mathbf{p}}_1 [\mathbf{0} \quad \mathbf{I} \quad \mathbf{0} \quad \mathbf{0}] \delta \mathbf{q}_g + \mathbf{R}_1^g \dot{\mathbf{r}}_2^0 \delta t \\ \delta \mathbf{p}_2 &= -\widetilde{\mathbf{p}}_2 [\mathbf{0} \quad \mathbf{0} \quad \mathbf{0} \quad \mathbf{I}] \delta \mathbf{q}_g + \mathbf{R}_2^g \dot{\mathbf{r}}_2^0 \delta t \end{aligned} \quad (\text{A.5})$$

Inserting Eq. (A.5) into Eq. (17), one obtains

$$\delta \mathbf{p} = -\frac{1}{2} [\mathbf{0} \quad \widetilde{\mathbf{p}}_1 \quad \mathbf{0} \quad \widetilde{\mathbf{p}}_2] \delta \mathbf{q}_g + \frac{\mathbf{R}_1^g + \mathbf{R}_2^g}{2} \dot{\mathbf{r}}_2^0 \delta t \quad (\text{A.6})$$

By taking the variation of Eq. (18), one obtains

$$\delta \mathbf{r}_3 = \frac{1}{\mathbf{r}_2^T \mathbf{p}} (\mathbf{I} - \mathbf{r}_3 \otimes \mathbf{r}_3) (-\mathbf{p} \times \delta \mathbf{r}_1 + \mathbf{r}_1 \times \delta \mathbf{p}) \quad (\text{A.7})$$

$$\delta \mathbf{r}_2 = -\mathbf{r}_1 \times \delta \mathbf{r}_3 + \mathbf{r}_3 \times \delta \mathbf{r}_1 \quad (\text{A.8})$$

Inserting Eqs. (A.3)-(A.8) into Eq. (54), one obtains

$$\begin{aligned}
-\mathbf{r}_2^T \delta \mathbf{r}_3 &= \frac{-\mathbf{r}_2^T}{\mathbf{r}_2^T \mathbf{p}} (\mathbf{I} - \mathbf{r}_3 \otimes \mathbf{r}_3) (-\mathbf{p} \times \delta \mathbf{r}_1 + \mathbf{r}_1 \times \delta \mathbf{p}) \\
&= \frac{\begin{bmatrix} \frac{2}{l_c} \mathbf{r}_1^T \mathbf{p} \mathbf{e}_3^T & \mathbf{r}_2^T \mathbf{p}_1 \mathbf{e}_1^T - \mathbf{r}_1^T \mathbf{p}_1 \mathbf{e}_2^T & -\frac{2}{l_c} \mathbf{r}_1^T \mathbf{p} \mathbf{e}_3^T & \mathbf{r}_2^T \mathbf{p}_2 \mathbf{e}_1^T - \mathbf{r}_1^T \mathbf{p}_2 \mathbf{e}_2^T \end{bmatrix}}{2\mathbf{r}_2^T \mathbf{p}} \mathbf{E}^T \delta \mathbf{q}_g \quad (\text{A.9}) \\
&+ \frac{-\mathbf{r}_1^T \mathbf{p} \mathbf{r}_3^T \frac{v_0 \mathbf{r}_1^0 + L \dot{\mathbf{r}}_1^0}{nl_c} + \mathbf{r}_3^T \frac{\mathbf{R}_1^g + \mathbf{R}_2^g}{2} \dot{\mathbf{r}}_2^0}{\mathbf{r}_2^T \mathbf{p}} \delta t
\end{aligned}$$

$$-\mathbf{r}_3^T \delta \mathbf{r}_1 = -\frac{\mathbf{e}_3^T}{l_c} [-\mathbf{I} \quad \mathbf{0} \quad \mathbf{I} \quad \mathbf{0}] \mathbf{E}^T \delta \mathbf{q}_g - \mathbf{r}_3^T \frac{v_0 \mathbf{r}_1^0 + L \dot{\mathbf{r}}_1^0}{nl_c} \delta t \quad (\text{A.10})$$

$$-\mathbf{r}_2^T \delta \mathbf{r}_1 = -\frac{\mathbf{e}_2^T}{l_c} [-\mathbf{I} \quad \mathbf{0} \quad \mathbf{I} \quad \mathbf{0}] \mathbf{E}^T \delta \mathbf{q}_g - \mathbf{r}_2^T \frac{v_0 \mathbf{r}_1^0 + L \dot{\mathbf{r}}_1^0}{nl_c} \delta t \quad (\text{A.11})$$

## Appendix B

Using Eqs. (42) and (67), the variation of  $\delta \mathbf{u}_g$  can be expressed as

$$\begin{aligned}
\delta \mathbf{u}_g &= \left[ N_1 (v \mathbf{R}_0 + L \dot{\mathbf{R}}_0) \frac{i-1}{n} \mathbf{e}_1 + N_2 (v \mathbf{R}_0 + L \dot{\mathbf{R}}_0) \frac{i}{n} \mathbf{e}_1 \right] \delta t + \dot{N}_1 \mathbf{X}_1 \delta t \\
&+ \dot{N}_2 \mathbf{X}_2 \delta t + \dot{N}_1 \mathbf{q}_g \delta t + N_1 \delta \mathbf{q}_g + \mathbf{R}_r \delta \mathbf{u}_l + \delta \mathbf{R}_r \mathbf{u}_l
\end{aligned} \quad (\text{B.1})$$

From Eqs. (41) and (59), by taking the variation of (69), one obtains

$$\begin{aligned}
\delta \mathbf{u}_l &= \dot{N}_2 \begin{bmatrix} \bar{\boldsymbol{\theta}}_1 \\ \bar{\boldsymbol{\theta}}_2 \end{bmatrix} \delta t + N_2 \begin{bmatrix} \mathbf{T}^{-1}(\bar{\boldsymbol{\theta}}_1) & \mathbf{0} \\ \mathbf{0} & \mathbf{T}^{-1}(\bar{\boldsymbol{\theta}}_2) \end{bmatrix} \delta \begin{bmatrix} \bar{\mathbf{w}}_1 \\ \bar{\mathbf{w}}_2 \end{bmatrix} \\
&\approx N_2 \mathbf{P}_1 \mathbf{E}^T \delta \mathbf{q}_g + \left( N_2 \mathbf{P}_2 + \dot{N}_2 \begin{bmatrix} \bar{\boldsymbol{\theta}}_1 \\ \bar{\boldsymbol{\theta}}_2 \end{bmatrix} \right) \delta t
\end{aligned} \quad (\text{B.2})$$

From Eqs. (46), (47) and (55),  $\delta \mathbf{R}_r \mathbf{u}_l$  can be rewritten as

$$\delta \mathbf{R}_r \mathbf{u}_l = \mathbf{R}_r \delta \widetilde{\mathbf{w}}_r^e \mathbf{u}_l = -\mathbf{R}_r \widetilde{\mathbf{u}}_l \delta \mathbf{w}_r^e = -\mathbf{R}_r \widetilde{\mathbf{u}}_l \mathbf{G}_1^T \mathbf{E}^T \delta \mathbf{q}_g - \mathbf{R}_r \widetilde{\mathbf{u}}_l \mathbf{G}_2^T \delta t \quad (\text{B.3})$$

Inserting Eqs. (B.2) and (B.3) into Eq. (B.1), one obtains

$$\begin{aligned} \mathbf{H}_1 = & N_1(v\mathbf{R}_0 + L\dot{\mathbf{R}}_0)\frac{i-1}{n}\mathbf{e}_1 + N_2(v\mathbf{R}_0 + L\dot{\mathbf{R}}_0)\frac{i}{n}\mathbf{e}_1 + \dot{N}_1\mathbf{X}_1 + \dot{N}_2\mathbf{X}_2 \\ & + \dot{N}_1\mathbf{q}_g + \mathbf{R}_r\dot{N}_2\begin{bmatrix}\bar{\boldsymbol{\theta}}_1 \\ \bar{\boldsymbol{\theta}}_2\end{bmatrix} + \mathbf{R}_rN_2\mathbf{P}_2 - \mathbf{R}_r\widetilde{\mathbf{u}}_l\mathbf{G}_2^T \end{aligned} \quad (\text{B.4})$$

$$\mathbf{H}_2 = N_1 + N_2\mathbf{P}_1 - \widetilde{\mathbf{u}}_l\mathbf{G}_1^T \quad (\text{B.5})$$

In Eqs. (B.4) and (B.5), the time derivative of the shape functions is evaluated as

$$\dot{N}_i = \frac{dN_i}{dt} = \frac{v}{n}\frac{\partial N_i}{\partial l_0} + \dot{\chi}\frac{\partial N_i}{\partial \chi} \quad (\text{B.6})$$

By taking the time first and second derivative of Eq. (25),  $\dot{\chi}$  and  $\ddot{\chi}$  are evaluated as

$$\begin{aligned} \dot{\chi} &= \left(1 - \frac{i-1}{n}\right)v \\ \ddot{\chi} &= \left(1 - \frac{i-1}{n}\right)a \end{aligned} \quad (\text{B.7})$$

Further,  $\ddot{N}_i$  can be expressed as

$$\ddot{N}_i = \frac{d\dot{N}_i}{dt} = \frac{v}{n}\frac{\partial \dot{N}_i}{\partial l_0} + \dot{\chi}\frac{\partial \dot{N}_i}{\partial \chi} + a\frac{\partial \dot{N}_i}{\partial v} + \ddot{\chi}\frac{\partial \dot{N}_i}{\partial \dot{\chi}} \quad (\text{B.8})$$

where  $a = dv/dt$ .

Assuming the local lateral displacement  $\widetilde{\mathbf{u}}_l$  is small [41] and taking the time derivative of Eq. (B.4), one obtains

$$\begin{aligned}
\dot{\mathbf{H}}_1 = & \left[ \dot{N}_1(v\mathbf{R}_0 + L\dot{\mathbf{R}}_0) \frac{i-1}{n} \mathbf{e}_1 + N_1(a\mathbf{R}_0 + 2v\dot{\mathbf{R}}_0 + L\ddot{\mathbf{R}}_0) \frac{i-1}{n} \mathbf{e}_1 \right] \\
& + \left[ \dot{N}_2(v\mathbf{R}_0 + L\dot{\mathbf{R}}_0) \frac{i}{n} \mathbf{e}_1 + N_2(a\mathbf{R}_0 + 2v\dot{\mathbf{R}}_0 + L\ddot{\mathbf{R}}_0) \frac{i}{n} \mathbf{e}_1 \right] \\
& + \left[ \dot{N}_1 \mathbf{X}_1 + \dot{N}_1(v\mathbf{R}_0 + L\dot{\mathbf{R}}_0) \frac{i-1}{n} \mathbf{e}_1 \right] \\
& + \left[ \dot{N}_2 \mathbf{X}_2 + \dot{N}_2(v\mathbf{R}_0 + L\dot{\mathbf{R}}_0) \frac{i}{n} \mathbf{e}_1 \right] + (\dot{N}_1 \mathbf{q}_g + \dot{N}_1 \dot{\mathbf{q}}_g) \\
& + \left[ \dot{\mathbf{R}}_r \dot{N}_2 \begin{bmatrix} \bar{\boldsymbol{\theta}}_1 \\ \bar{\boldsymbol{\theta}}_2 \end{bmatrix} + \mathbf{R}_r \ddot{N}_2 \begin{bmatrix} \bar{\boldsymbol{\theta}}_1 \\ \bar{\boldsymbol{\theta}}_2 \end{bmatrix} + \mathbf{R}_r \dot{N}_2 (\mathbf{P}_1 \mathbf{E}^T \dot{\mathbf{q}}_g + \mathbf{P}_2) \right] \\
& + (\dot{\mathbf{R}}_r \mathbf{N}_2 \mathbf{P}_2 + \mathbf{R}_r \dot{N}_2 \mathbf{P}_2 + \mathbf{R}_r \mathbf{N}_2 \dot{\mathbf{P}}_2) - \mathbf{R}_r \widetilde{\mathbf{u}}_l \mathbf{G}_2^T
\end{aligned} \tag{B.9}$$

where  $\mathbf{u}_l$  can be obtained from Eq. (B.2). By taking the time derivative of Eq. (59),  $\dot{\mathbf{P}}_2$  is expressed as

$$\dot{\mathbf{P}}_2 = \begin{bmatrix} -\dot{\mathbf{G}}_2^T + \ddot{\mathbf{w}}_0^1 \\ -\dot{\mathbf{G}}_2^T + \ddot{\mathbf{w}}_0^2 \end{bmatrix} \tag{B.10}$$

where  $\dot{\mathbf{G}}_2^T$  and  $\ddot{\mathbf{w}}_0^k$  are obtained by taking the time derivative of Eqs. (58) and (51), i.e.

$$\dot{\mathbf{G}}_2^T = \begin{bmatrix} \frac{d}{dt} \left( \frac{-(\mathbf{p} \cdot \mathbf{r}_1) \mathbf{e}_3^T \mathbf{R}_r^T \frac{v_0 \mathbf{r}_1^0 + L \dot{\mathbf{r}}_1^0}{nl_c} + \mathbf{e}_3^T \frac{\bar{\mathbf{R}}_1 + \bar{\mathbf{R}}_2}{2} \mathbf{R}_0^T \dot{\mathbf{r}}_2^0}{\mathbf{r}_2 \cdot \mathbf{p}} \right) \\ -\mathbf{e}_3^T \dot{\mathbf{R}}_r^T \frac{v_0 \mathbf{r}_1^0 + L \dot{\mathbf{r}}_1^0}{nl_c} - \mathbf{e}_3^T \mathbf{R}_r^T \frac{a_0 \mathbf{r}_1^0 + 2v_0 \dot{\mathbf{r}}_1^0 + L \ddot{\mathbf{r}}_1^0}{nl_c} + \mathbf{e}_3^T \mathbf{R}_r^T \frac{v_0 \mathbf{r}_1^0 + L \dot{\mathbf{r}}_1^0}{nl_c^2} l_c \\ -\mathbf{e}_2^T \dot{\mathbf{R}}_r^T \frac{v_0 \mathbf{r}_1^0 + L \dot{\mathbf{r}}_1^0}{nl_c} - \mathbf{e}_2^T \mathbf{R}_r^T \frac{a_0 \mathbf{r}_1^0 + 2v_0 \dot{\mathbf{r}}_1^0 + L \ddot{\mathbf{r}}_1^0}{nl_c} + \mathbf{e}_2^T \mathbf{R}_r^T \frac{v_0 \mathbf{r}_1^0 + L \dot{\mathbf{r}}_1^0}{nl_c^2} l_c \end{bmatrix} \tag{B.11}$$

$$\ddot{\mathbf{w}}_0^k = \widetilde{\mathbf{w}}_k \bar{\mathbf{R}}_k \text{vect}(\mathbf{R}_0^T \dot{\mathbf{R}}_0) + \bar{\mathbf{R}}_k \text{vect}(\dot{\mathbf{R}}_0^T \dot{\mathbf{R}}_0 + \mathbf{R}_0^T \ddot{\mathbf{R}}_0), \quad k = 1, 2. \tag{B.12}$$

where  $\dot{l}_c$  and  $\dot{\mathbf{w}}_k$  can be obtained using Eqs. (43) and (50).

Considering the local lateral displacement  $\widetilde{\mathbf{u}}_l$  is small [41] and taking the time derivative of Eq. (B.5), one obtains

$$\dot{\mathbf{H}}_2 = \dot{\mathbf{N}}_1 + \dot{\mathbf{N}}_2 \mathbf{P}_1 + \mathbf{N}_2 \dot{\mathbf{P}}_1 - \widetilde{\mathbf{u}}_l \mathbf{G}_1^T \quad (\text{B.13})$$

where  $\dot{\mathbf{P}}_1$  can be obtained using Eq. (59), i.e.

$$\dot{\mathbf{P}}_1 = - \begin{bmatrix} \dot{\mathbf{G}}_1^T \\ \dot{\mathbf{G}}_1^T \end{bmatrix} \quad (\text{B.14})$$

By taking the time derivative of Eq. (56), one obtains

$$\begin{aligned} & \dot{\mathbf{G}}_1^T \\ &= \begin{bmatrix} 0 & 0 & \frac{\dot{\eta}}{l_c} - \eta \frac{\dot{l}_c}{l_c^2} & \frac{\dot{\eta}_{12}}{2} & -\frac{\dot{\eta}_{11}}{2} & 0 & 0 & 0 & \eta \frac{\dot{l}_c}{l_c^2} - \frac{\dot{\eta}}{l_c} & \frac{\dot{\eta}_{22}}{2} & -\frac{\dot{\eta}_{21}}{2} & 0 \\ 0 & 0 & -\frac{\dot{l}_c}{l_c^2} & 0 & 0 & 0 & 0 & 0 & \frac{\dot{l}_c}{l_c^2} & 0 & 0 & 0 \\ 0 & \frac{\dot{l}_c}{l_c^2} & 0 & 0 & 0 & 0 & 0 & -\frac{\dot{l}_c}{l_c^2} & 0 & 0 & 0 & 0 \end{bmatrix} \quad (\text{B.15}) \end{aligned}$$

where  $\dot{\eta}$ ,  $\dot{\eta}_{k1}$  and  $\dot{\eta}_{k2}$  can be obtained by taking the variation of Eqs. (57), i.e.

$$\delta\eta = \frac{\mathbf{p}^T \delta \mathbf{r}_1 + \mathbf{r}_1^T \delta \mathbf{p}}{\mathbf{p}^T \mathbf{r}_2} - \eta \frac{\mathbf{p}^T \delta \mathbf{r}_2 + \mathbf{r}_2^T \delta \mathbf{p}}{\mathbf{p}^T \mathbf{r}_2} \quad (\text{B.16})$$

$$\delta\eta_{k1} = \frac{\mathbf{p}_k^T \delta \mathbf{r}_1 + \mathbf{r}_1^T \delta \mathbf{p}_k}{\mathbf{p}^T \mathbf{r}_2} - \eta_{k1} \frac{\mathbf{p}^T \delta \mathbf{r}_2 + \mathbf{r}_2^T \delta \mathbf{p}}{\mathbf{p}^T \mathbf{r}_2} \quad (\text{B.17})$$

$$\delta\eta_{k2} = \frac{\mathbf{p}_k^T \delta \mathbf{r}_2 + \mathbf{r}_2^T \delta \mathbf{p}_k}{\mathbf{p}^T \mathbf{r}_2} - \eta_{k2} \frac{\mathbf{p}^T \delta \mathbf{r}_2 + \mathbf{r}_2^T \delta \mathbf{p}}{\mathbf{p}^T \mathbf{r}_2} \quad (\text{B.18})$$

Inserting Eqs. (B.14) and (B.15) into Eq. (B.13),  $\dot{\mathbf{H}}_2$  can be rewritten as

$$\dot{\mathbf{H}}_2 = \dot{\mathbf{N}}_1 + \dot{\mathbf{N}}_2 \begin{bmatrix} \mathbf{0} & \mathbf{I} & \mathbf{0} & \mathbf{0} \\ \mathbf{0} & \mathbf{0} & \mathbf{0} & \mathbf{I} \end{bmatrix} - \frac{1}{l_c} \dot{\mathbf{N}}_2 \begin{bmatrix} \mathbf{I} \\ \mathbf{I} \end{bmatrix} \mathbf{N}_4 + \frac{\dot{l}_c}{l_c^2} \mathbf{N}_2 \begin{bmatrix} \mathbf{I} \\ \mathbf{I} \end{bmatrix} \mathbf{N}_4 - \widetilde{\mathbf{u}}_l \mathbf{G}_1^T \quad (\text{B.19})$$

with

$$\mathbf{N}_4 = \begin{bmatrix} 0 & 0 & 0 & 0 & 0 & 0 & 0 & 0 & 0 & 0 & 0 & 0 \\ 0 & 0 & 1 & 0 & 0 & 0 & 0 & 0 & -1 & 0 & 0 & 0 \\ 0 & -1 & 0 & 0 & 0 & 0 & 0 & 1 & 0 & 0 & 0 & 0 \end{bmatrix} \quad (\text{B.20})$$

From Eqs. (46) and (47),  $\dot{\mathbf{R}}_r$  is obtained as

$$\dot{\mathbf{R}}_r = \mathbf{R}_r \widetilde{\dot{\mathbf{w}}}_r^e \quad (\text{B.21})$$

where  $\widetilde{\dot{\mathbf{w}}}_r^e$  is obtained using Eq. (55). Using Eq. (B.21), and taking the time derivative of Eq. (52), one obtains

$$\dot{\mathbf{E}} = \mathbf{E} \begin{bmatrix} \widetilde{\dot{\mathbf{w}}}_r^e & \mathbf{0} & \mathbf{0} & \mathbf{0} \\ \mathbf{0} & \widetilde{\dot{\mathbf{w}}}_r^e & \mathbf{0} & \mathbf{0} \\ \mathbf{0} & \mathbf{0} & \widetilde{\dot{\mathbf{w}}}_r^e & \mathbf{0} \\ \mathbf{0} & \mathbf{0} & \mathbf{0} & \widetilde{\dot{\mathbf{w}}}_r^e \end{bmatrix} = \mathbf{E} \dot{\mathbf{E}}_r, \quad \mathbf{E}_r = \begin{bmatrix} \widetilde{\dot{\mathbf{w}}}_r^e & \mathbf{0} & \mathbf{0} & \mathbf{0} \\ \mathbf{0} & \widetilde{\dot{\mathbf{w}}}_r^e & \mathbf{0} & \mathbf{0} \\ \mathbf{0} & \mathbf{0} & \widetilde{\dot{\mathbf{w}}}_r^e & \mathbf{0} \\ \mathbf{0} & \mathbf{0} & \mathbf{0} & \widetilde{\dot{\mathbf{w}}}_r^e \end{bmatrix} \quad (\text{B.22})$$

## Appendix C

From Eq. (B.9),  $\mathbf{R}_r^T \widehat{\mathbf{H}}_1$  can be expanded as

$$\begin{aligned}
\mathbf{R}_r^T \widehat{\mathbf{H}}_1 = & \mathbf{R}_r^T \ddot{\mathbf{N}}_1 + \left[ - \left( \widetilde{\dot{\mathbf{w}}_r^e \dot{\mathbf{N}}_2} \begin{bmatrix} \overline{\boldsymbol{\theta}}_1 \\ \overline{\boldsymbol{\theta}}_2 \end{bmatrix} \right) \widehat{\mathbf{w}}_r^e - \left( \dot{\mathbf{N}}_2 \begin{bmatrix} \overline{\boldsymbol{\theta}}_1 \\ \overline{\boldsymbol{\theta}}_2 \end{bmatrix} \right) \widehat{\mathbf{w}}_r^e + \widetilde{\dot{\mathbf{w}}_r^e \dot{\mathbf{N}}_2} \mathbf{P}_1 \mathbf{E}^T \right] \\
& + \left[ - \left( \dot{\mathbf{N}}_2 \begin{bmatrix} \overline{\boldsymbol{\theta}}_1 \\ \overline{\boldsymbol{\theta}}_2 \end{bmatrix} \right) \widehat{\mathbf{w}}_r^e + \ddot{\mathbf{N}}_2 \mathbf{P}_1 \mathbf{E}^T \right] \\
& + \left[ - (\dot{\mathbf{N}}_2 \mathbf{P}_1 \mathbf{Q}_1 + \dot{\mathbf{N}}_2 \mathbf{P}_2) \widehat{\mathbf{w}}_r^e + \frac{1}{l_c^2} \dot{\mathbf{N}}_2 \begin{bmatrix} \mathbf{I} \\ \mathbf{I} \end{bmatrix} \mathbf{N}_4 \mathbf{Q}_1 \bar{\mathbf{U}} \right. \\
& \left. - \dot{\mathbf{N}}_2 \mathbf{P}_1 \widehat{\mathbf{E}}_r \mathbf{Q}_1 + (\dot{\mathbf{N}}_2 \mathbf{P}_2) \right] \\
& + \left[ - (\widetilde{\dot{\mathbf{w}}_r^e \dot{\mathbf{N}}_2 \mathbf{P}_2}) \widehat{\mathbf{w}}_r^e - (\dot{\mathbf{N}}_2 \mathbf{P}_2) \widehat{\mathbf{w}}_r^e + \widetilde{\dot{\mathbf{w}}_r^e (\dot{\mathbf{N}}_2 \mathbf{P}_2)} - (\dot{\mathbf{N}}_2 \mathbf{P}_2) \widehat{\mathbf{w}}_r^e \right. \\
& \left. + (\dot{\mathbf{N}}_2 \mathbf{P}_2) - (\dot{\mathbf{N}}_2 \dot{\mathbf{P}}_2) \widehat{\mathbf{w}}_r^e + (\dot{\mathbf{N}}_2 \dot{\mathbf{P}}_2) \right] \\
& - \left[ - (\widetilde{\dot{\mathbf{u}}_l \mathbf{G}_2^T}) \widehat{\mathbf{w}}_r^e + \widetilde{\dot{\mathbf{u}}_l \mathbf{G}_2^T} - \mathbf{G}_2^T \widehat{\mathbf{u}}_l \right]
\end{aligned} \tag{C.1}$$

$\widehat{\mathbf{w}}_r^e$ ,  $\widehat{\mathbf{u}}_l$ ,  $(\dot{\mathbf{N}}_2 \mathbf{P}_2)$ ,  $(\dot{\mathbf{N}}_2 \dot{\mathbf{P}}_2)$ ,  $\mathbf{G}_2^T$  and  $(\dot{\mathbf{N}}_2 \dot{\mathbf{P}}_2)$  can be obtained using Eqs. (55),

(B.2), (59), (58) and (B.10).

$$\widehat{\mathbf{w}}_r^e = \mathbf{G}_1^T \mathbf{Q}_1 - \mathbf{G}_1^T \widehat{\mathbf{E}}_r \mathbf{Q}_1 + \mathbf{G}_2^T \tag{C.2}$$

$$\widehat{\mathbf{u}}_l = \dot{\mathbf{N}}_2 \mathbf{P}_1 \mathbf{E}^T + \frac{1}{l_c^2} \dot{\mathbf{N}}_2 \begin{bmatrix} \mathbf{I} \\ \mathbf{I} \end{bmatrix} \mathbf{N}_4 \mathbf{Q}_1 \bar{\mathbf{U}} - \dot{\mathbf{N}}_2 \mathbf{P}_1 \widehat{\mathbf{E}}_r \mathbf{Q}_1 + (\dot{\mathbf{N}}_2 \mathbf{P}_2) \tag{C.3}$$

$$(\dot{\mathbf{N}}_2 \mathbf{P}_2) = \frac{\partial}{\partial \dot{\mathbf{q}}_g} (\dot{\mathbf{N}}_2 \dot{\mathbf{P}}_2) = -\dot{\mathbf{N}}_2 \begin{bmatrix} \mathbf{I} \\ \mathbf{I} \end{bmatrix} \begin{bmatrix} \mathbf{0}_{1 \times 12} \\ \widehat{\mathbf{G}}_2^2 \\ \widehat{\mathbf{G}}_2^3 \end{bmatrix} + \dot{\mathbf{N}}_2 \begin{bmatrix} \widehat{\mathbf{w}}_0^1 \\ \widehat{\mathbf{w}}_0^2 \end{bmatrix} \tag{C.4}$$

$$(\dot{\mathbf{N}}_2 \dot{\mathbf{P}}_2) = -\dot{\mathbf{N}}_2 \begin{bmatrix} \mathbf{I} \\ \mathbf{I} \end{bmatrix} \begin{bmatrix} \mathbf{0}_{1 \times 12} \\ \widehat{\mathbf{G}}_2^2 \\ \widehat{\mathbf{G}}_2^3 \end{bmatrix} + \dot{\mathbf{N}}_2 \begin{bmatrix} \widehat{\mathbf{w}}_0^1 \\ \widehat{\mathbf{w}}_0^2 \end{bmatrix} \tag{C.5}$$



$$\widehat{\mathbf{G}}_2^T = \begin{bmatrix} \widehat{G}_2^1 \\ \widehat{G}_2^2 \\ \widehat{G}_2^3 \end{bmatrix} = \begin{bmatrix} \widehat{G}_2^1 \\ -\mathbf{e}_3^T \left( \mathbf{R}_r^T \frac{v_0 \widetilde{\mathbf{r}_1^0} + L \dot{\mathbf{r}}_1^0}{nl_c} \right) \mathbf{G}_1^T \mathbf{E}^T + \mathbf{e}_3^T \mathbf{R}_r^T \frac{v_0 \mathbf{r}_1^0 + L \dot{\mathbf{r}}_1^0}{nl_c^2} \bar{\mathbf{U}} \\ -\mathbf{e}_2^T \left( \mathbf{R}_r^T \frac{v_0 \widetilde{\mathbf{r}_1^0} + L \dot{\mathbf{r}}_1^0}{nl_c} \right) \mathbf{G}_1^T \mathbf{E}^T + \mathbf{e}_2^T \mathbf{R}_r^T \frac{v_0 \mathbf{r}_1^0 + L \dot{\mathbf{r}}_1^0}{nl_c^2} \bar{\mathbf{U}} \end{bmatrix} \quad (\text{C.6})$$

$$(\widehat{N_2 \dot{\mathbf{P}}_2}) = -N_2 \begin{bmatrix} \mathbf{I} \\ \mathbf{I} \end{bmatrix} \begin{bmatrix} \mathbf{0}_{1 \times 12} \\ \widehat{G}_2^2 \\ \widehat{G}_2^3 \end{bmatrix} + N_2 \begin{bmatrix} \widehat{\mathbf{w}}_0^1 \\ \widehat{\mathbf{w}}_0^2 \end{bmatrix} \quad (\text{C.7})$$

$\widehat{\mathbf{w}}_0^k$ ,  $\widehat{G}_2^1$ ,  $\widehat{G}_2^2$ ,  $\widehat{G}_2^3$  and  $\widehat{\mathbf{w}}_0^k (k = 1, 2)$  can be obtained using Eqs. (51), (58), (B.11) and (B.12).

$$\widehat{\mathbf{w}}_0^k = \frac{\partial \dot{\mathbf{w}}_0^k}{\partial \dot{\mathbf{q}}_g} = - \left( \bar{\mathbf{R}}_k \text{vect}(\widetilde{\mathbf{R}_0^T \dot{\mathbf{R}}_0}) \right) [\delta_{1k} \mathbf{I} \quad \delta_{2k} \mathbf{I}] \mathbf{P}_1 \mathbf{E}^T, \quad k = 1, 2. \quad (\text{C.8})$$

$$\begin{aligned} \widehat{G}_2^1 = & -\mathbf{e}_3^T \mathbf{R}_r^T \frac{v_0 \mathbf{r}_1^0 + L \dot{\mathbf{r}}_1^0}{nl_c} \hat{\eta} - \eta \mathbf{e}_3^T \left( \mathbf{R}_r^T \frac{v_0 \widetilde{\mathbf{r}_1^0} + L \dot{\mathbf{r}}_1^0}{nl_c} \right) \mathbf{G}_1^T \mathbf{E}^T \\ & + \eta \mathbf{e}_3^T \mathbf{R}_r^T \frac{v_0 \mathbf{r}_1^0 + L \dot{\mathbf{r}}_1^0}{nl_c^2} \bar{\mathbf{U}} \\ & - \frac{\mathbf{e}_3^T (\bar{\mathbf{R}}_1 \widetilde{\mathbf{R}_0^T \dot{\mathbf{r}}_2^0})}{2 \mathbf{r}_2 \cdot \mathbf{p}} ([\mathbf{0} \quad \mathbf{I} \quad \mathbf{0} \quad \mathbf{0}] - \mathbf{G}_1^T) \mathbf{E}^T \\ & - \frac{\mathbf{e}_3^T (\bar{\mathbf{R}}_2 \widetilde{\mathbf{R}_0^T \dot{\mathbf{r}}_2^0})}{2 \mathbf{r}_2 \cdot \mathbf{p}} ([\mathbf{0} \quad \mathbf{0} \quad \mathbf{0} \quad \mathbf{I}] - \mathbf{G}_1^T) \mathbf{E}^T \\ & - \frac{\mathbf{e}_3^T (\bar{\mathbf{R}}_1 + \bar{\mathbf{R}}_2) \mathbf{R}_0^T \dot{\mathbf{r}}_2^0}{2 (\mathbf{r}_2 \cdot \mathbf{p})^2} (\mathbf{p}^T \hat{\mathbf{r}}_2 + \mathbf{r}_2^T \hat{\mathbf{p}}) \end{aligned} \quad (\text{C.9})$$

$$\begin{aligned}
\hat{G}_2^j = & (\delta_{2j}\mathbf{e}_3^T + \delta_{3j}\mathbf{e}_2^T) \left[ - \left( \mathbf{R}_r^T \frac{\widetilde{v_0 \mathbf{r}_1^0 + L \dot{\mathbf{r}}_1^0}}{nl_c} \right) \widehat{\mathbf{w}}_r^e \right. \\
& + \widehat{\mathbf{w}}_r^e \left( \mathbf{R}_r^T \frac{\widetilde{v_0 \mathbf{r}_1^0 + L \dot{\mathbf{r}}_1^0}}{nl_c} \right) \widehat{\mathbf{w}}_r^e + \dot{\mathbf{R}}_r^T \frac{v_0 \mathbf{r}_1^0 + L \dot{\mathbf{r}}_1^0}{nl_c^2} \bar{\mathbf{U}} \\
& - \left( \mathbf{R}_r^T \frac{a_0 \mathbf{r}_1^0 + 2v_0 \dot{\mathbf{r}}_1^0 + L \ddot{\mathbf{r}}_1^0}{nl_c} \right) \widehat{\mathbf{w}}_r^e \\
& + \mathbf{R}_r^T \frac{a_0 \mathbf{r}_1^0 + 2v_0 \dot{\mathbf{r}}_1^0 + L \ddot{\mathbf{r}}_1^0}{nl_c^2} \bar{\mathbf{U}} + \left( \mathbf{R}_r^T \frac{\widetilde{v_0 \mathbf{r}_1^0 + L \dot{\mathbf{r}}_1^0}}{nl_c^2} \hat{l}_c \right) \widehat{\mathbf{w}}_r^e \\
& \left. - 2\mathbf{R}_r^T \frac{v_0 \mathbf{r}_1^0 + L \dot{\mathbf{r}}_1^0}{nl_c^3} \hat{l}_c \bar{\mathbf{U}} + \mathbf{R}_r^T \frac{v_0 \mathbf{r}_1^0 + L \dot{\mathbf{r}}_1^0}{nl_c^2} \hat{l}_c \right], \quad j = 2, 3.
\end{aligned} \tag{C.10}$$

$$\begin{aligned}
\widehat{\mathbf{w}}_0^k = & - \left[ \widehat{\mathbf{w}}_k \left( \bar{\mathbf{R}}_k \text{vect}(\widetilde{\mathbf{R}_0^T \dot{\mathbf{R}}_0}) \right) + \left( \bar{\mathbf{R}}_k \text{vect}(\widetilde{\dot{\mathbf{R}}_0^T \dot{\mathbf{R}}_0 + \mathbf{R}_0^T \ddot{\mathbf{R}}_0}) \right) \right] \widehat{\mathbf{w}}_k \\
& - \left( \bar{\mathbf{R}}_k \text{vect}(\widetilde{\mathbf{R}_0^T \dot{\mathbf{R}}_0}) \right) \widehat{\mathbf{w}}_k
\end{aligned} \tag{C.11}$$

where  $\delta_{ij} = \begin{cases} 1, & i = j \\ 0, & i \neq j \end{cases}$ . The quantities  $\hat{\mathbf{p}}$ ,  $\hat{\mathbf{r}}_2$ ,  $\hat{\eta}$  and  $\widehat{\mathbf{w}}_k$  in Eqs. (C.9) and (C.10) can be obtained using Eqs. (A.6), (A.8), (B.16) and (59), respectively. Using Eqs. (43) and (59),  $\hat{l}_c$  and  $\widehat{\mathbf{w}}_k$  can be expressed as

$$\hat{l}_c = \dot{\mathbf{q}}_g^T \widehat{\mathbf{U}}^T + \frac{v_0 \mathbf{r}_1^0 + L \dot{\mathbf{r}}_1^0}{n} \hat{\mathbf{r}}_1 \tag{C.12}$$

$$\widehat{\mathbf{w}}_k = -\widehat{\mathbf{G}}_1^T \mathbf{Q}_1 - [\delta_{1k} \mathbf{I} \quad \delta_{2k} \mathbf{I}] \mathbf{P}_1 \widehat{\mathbf{E}}_r \mathbf{Q}_1 - \widehat{\mathbf{G}}_2^T + \widehat{\mathbf{w}}_0^k \tag{C.13}$$

From Eqs. (92), (B.2) and (B.9), one obtains

$$\begin{aligned} \frac{\partial \dot{H}_1}{\partial \dot{q}} = \hat{H}_1 = \dot{N}_1 - R_r \left( \dot{N}_2 \left[ \begin{array}{c} \bar{\theta}_1 \\ \bar{\theta}_2 \end{array} \right] + N_2 P_2 \right) G_1^T E^T + R_r \dot{N}_2 P_1 E^T \\ + R_r \frac{\partial}{\partial \dot{q}_g} (N_2 \dot{P}_2) + R_r \widetilde{G}_2^T N_2 P_1 E^T \end{aligned} \quad (C.14)$$

where  $\frac{\partial}{\partial \dot{q}_g} (N_2 \dot{P}_2)$  has been given by Eq. (C.4).

From Eq. (82),  $\widehat{\mathbf{w}}_e$  can be expanded as

$$\begin{aligned} \widehat{\mathbf{w}}_e = -(\widetilde{H_3 Q_1}) \widehat{\mathbf{w}}_r^e + \widetilde{\mathbf{w}}_r^e \widehat{H}_3 Q_1 + \widehat{H}_3 Q_1 + \widehat{H}_3 Q_6 - H_3 \widehat{E}_r Q_1 \\ - (\widetilde{\mathbf{w}}_r^e H_3 + \dot{H}_3 - H_3 \dot{E}_r) \widehat{E}_r Q_1 + (\widehat{H}_3 - H_3 \widehat{E}_r) Q_7 \\ + \widetilde{H}_4 \widehat{\mathbf{w}}_r^e + \widetilde{\mathbf{w}}_r^e \widehat{H}_4 + \widehat{H}_4 \end{aligned} \quad (C.15)$$

where  $\widehat{H}_4$  and  $\widehat{\widetilde{H}}_4$  can be obtained using Eqs. (80) and (84), respectively

$$\widehat{H}_4 = \frac{\partial \dot{H}_4}{\partial \dot{q}_g} = \left( I - N_3 \begin{bmatrix} I \\ I \end{bmatrix} \right) \begin{bmatrix} \mathbf{0}_{1 \times 12} \\ \widehat{G}_2^2 \\ \widehat{G}_2^3 \end{bmatrix} + N_3 \begin{bmatrix} \widehat{\mathbf{w}}_0^1 \\ \widehat{\mathbf{w}}_0^2 \end{bmatrix} + \dot{N}_3 P_1 E^T \quad (C.16)$$

$$\begin{aligned} \widehat{\widetilde{H}}_4 = \left( I - N_3 \begin{bmatrix} I \\ I \end{bmatrix} \right) \begin{bmatrix} \mathbf{0}_{1 \times 12} \\ \widehat{G}_2^2 \\ \widehat{G}_2^3 \end{bmatrix} + N_3 \begin{bmatrix} \widehat{\mathbf{w}}_0^1 \\ \widehat{\mathbf{w}}_0^2 \end{bmatrix} + \ddot{N}_3 P_1 E^T + \frac{1}{l_c^2} \dot{N}_3 \begin{bmatrix} I \\ I \end{bmatrix} N_4 Q_1 \bar{U} \\ - \dot{N}_3 P_1 \widehat{E}_r Q_1 - 2 \dot{N}_3 \begin{bmatrix} I \\ I \end{bmatrix} \begin{bmatrix} \mathbf{0}_{1 \times 12} \\ \widehat{G}_2^2 \\ \widehat{G}_2^3 \end{bmatrix} + 2 \dot{N}_3 \begin{bmatrix} \widehat{\mathbf{w}}_0^1 \\ \widehat{\mathbf{w}}_0^2 \end{bmatrix} \end{aligned} \quad (C.17)$$

$\widehat{\mathbf{w}}_e$ ,  $\widehat{\boldsymbol{\theta}}$  and  $\widehat{\boldsymbol{\Omega}}$  can be obtained using Eqs. (81), (74) and (63), respectively

$$\widehat{\mathbf{w}}_e = \widehat{H}_3 Q_1 - H_3 \widehat{E}_r Q_1 + \widehat{H}_4 \quad (C.18)$$

$$\widehat{\boldsymbol{\theta}} = N_3 P_1 E^T \quad (C.19)$$

$$\widehat{\boldsymbol{\Omega}} = \widetilde{\boldsymbol{w}}_e \widehat{\boldsymbol{\theta}} + \overline{\boldsymbol{R}}^T \widehat{\boldsymbol{w}}_e \quad (\text{C.20})$$

Using Eq. (B.13), one obtains

$$\begin{aligned} \widehat{\boldsymbol{H}}_2 \boldsymbol{Q}_1 &= \frac{1}{l_c^2} \dot{N}_2 \begin{bmatrix} \boldsymbol{I} \\ \boldsymbol{I} \end{bmatrix} N_4 \boldsymbol{Q}_1 \bar{U} - \frac{2}{l_c^3} N_2 \begin{bmatrix} \boldsymbol{I} \\ \boldsymbol{I} \end{bmatrix} N_4 \boldsymbol{Q}_1 \bar{U} + \frac{1}{l_c^2} N_2 \begin{bmatrix} \boldsymbol{I} \\ \boldsymbol{I} \end{bmatrix} N_4 \boldsymbol{Q}_1 \hat{l}_c \\ &\quad + (\widetilde{\boldsymbol{G}_1^T \boldsymbol{Q}_1}) \widehat{\boldsymbol{u}}_l - \widetilde{\boldsymbol{u}}_l \widehat{\boldsymbol{G}}_1^T \boldsymbol{Q}_1 \end{aligned} \quad (\text{C.21})$$

where  $\hat{l}_c$  and  $\widehat{\boldsymbol{u}}_l$  can be obtained using Eqs. (C.12) and (C.3), respectively.

$$\widehat{\boldsymbol{H}}_2 \boldsymbol{Q}_k = \frac{\partial \dot{\boldsymbol{H}}_2}{\partial \dot{\boldsymbol{q}}_g} \boldsymbol{Q}_k = \frac{1}{l_c^2} N_2 \begin{bmatrix} \boldsymbol{I} \\ \boldsymbol{I} \end{bmatrix} N_4 \boldsymbol{Q}_k \bar{U} + (\widetilde{\boldsymbol{G}_1^T \boldsymbol{Q}_k}) \widehat{\boldsymbol{u}}_l - \widetilde{\boldsymbol{u}}_l \widehat{\boldsymbol{G}}_1^T \boldsymbol{Q}_k, \quad k = 1, 6, 7. \quad (\text{C.22})$$

$$\widehat{\boldsymbol{H}}_2^T \boldsymbol{Q}_5 = \widehat{\boldsymbol{P}}_1^T \boldsymbol{Q}_{10} + \widehat{\boldsymbol{G}}_1 \boldsymbol{Q}_{11} - \boldsymbol{G}_1 \widetilde{\boldsymbol{Q}}_5 \widehat{\boldsymbol{u}}_l \quad (\text{C.23})$$

with

$$\boldsymbol{Q}_{10} = N_2^T \boldsymbol{Q}_5, \quad \boldsymbol{Q}_{11} = \widetilde{\boldsymbol{u}}_l \boldsymbol{Q}_5 \quad (\text{C.24})$$

$\widehat{\boldsymbol{H}}_3 \boldsymbol{Q}_1$  can be obtained using Eq. (83)

$$\begin{aligned} \widehat{\boldsymbol{H}}_3 \boldsymbol{Q}_1 &= \frac{1}{l_c^2} \left( N_3 \begin{bmatrix} \boldsymbol{I} \\ \boldsymbol{I} \end{bmatrix} - \boldsymbol{I} \right) N_4 \boldsymbol{Q}_1 \hat{l}_c - \frac{2\dot{l}_c}{l_c^3} \left( N_3 \begin{bmatrix} \boldsymbol{I} \\ \boldsymbol{I} \end{bmatrix} - \boldsymbol{I} \right) N_4 \boldsymbol{Q}_1 \bar{U} \\ &\quad + \frac{1}{l_c^2} \dot{N}_3 \begin{bmatrix} \boldsymbol{I} \\ \boldsymbol{I} \end{bmatrix} N_4 \boldsymbol{Q}_1 \bar{U} \end{aligned} \quad (\text{C.25})$$

Using Eq. (79), one obtains

$$\widehat{\boldsymbol{H}}_3 \boldsymbol{Q}_k = \frac{\partial \dot{\boldsymbol{H}}_3}{\partial \dot{\boldsymbol{q}}} \boldsymbol{Q}_k = -\frac{1}{l_c^2} \left( \boldsymbol{I} - N_3 \begin{bmatrix} \boldsymbol{I} \\ \boldsymbol{I} \end{bmatrix} \right) N_4 \boldsymbol{Q}_k \bar{U}, \quad k = 1, 6, 7 \quad (\text{C.26})$$

$$\hat{\mathbf{H}}_3^T \mathbf{Q}_9 = -\frac{1}{l_c^2} \mathbf{N}_4^T (\mathbf{I} - [\mathbf{I} \quad \mathbf{I}] \mathbf{N}_3^T) \mathbf{Q}_9 \bar{\mathbf{U}} \quad (\text{C.27})$$

Using Eq. (59), one obtains

$$\hat{\mathbf{P}}_1^T \mathbf{Q}_k = -\hat{\mathbf{G}}_1 \mathbf{Q}_k^1 - \hat{\mathbf{G}}_1 \mathbf{Q}_k^2, \quad k = 2, 10 \quad (\text{C.28})$$

with

$$\mathbf{Q}_2 = \begin{bmatrix} \mathbf{Q}_2^1 \\ \mathbf{Q}_2^2 \end{bmatrix} = \begin{bmatrix} \mathbf{Q}_{12} \\ \mathbf{Q}_{13} \end{bmatrix}, \quad \mathbf{Q}_{10} = \begin{bmatrix} \mathbf{Q}_{10}^1 \\ \mathbf{Q}_{10}^2 \end{bmatrix} = \begin{bmatrix} \mathbf{Q}_{14} \\ \mathbf{Q}_{15} \end{bmatrix} \quad (\text{C.29})$$

$\hat{\mathbf{G}}_1 \mathbf{Q}_k (k = 11, \dots, 15)$  can be obtained using Eq. (56)

$$\hat{\mathbf{G}}_1 \mathbf{Q}_k = -\frac{1}{l_c^2} \mathbf{N}_4^T \begin{bmatrix} 0 \\ \eta \mathbf{Q}_k^1 + \mathbf{Q}_k^2 \\ \mathbf{Q}_k^3 \end{bmatrix} \bar{\mathbf{U}} + \mathbf{Q}_k^1 \mathbf{A}, \quad k = 11, \dots, 15. \quad (\text{C.30})$$

with  $\mathbf{Q}_k = [\mathbf{Q}_k^1 \quad \mathbf{Q}_k^2 \quad \mathbf{Q}_k^3]^T (k = 11, \dots, 15)$  and

$$\mathbf{A} = \begin{bmatrix} \mathbf{0}_{12 \times 2} & \frac{\hat{\eta}}{l_c} & \frac{\hat{\eta}_{12}}{2} & -\frac{\hat{\eta}_{11}}{2} & \mathbf{0}_{12 \times 3} & -\frac{\hat{\eta}}{l_c} & \frac{\hat{\eta}_{22}}{2} & -\frac{\hat{\eta}_{21}}{2} & \mathbf{0}_{12 \times 1} \end{bmatrix}^T \quad (\text{C.31})$$

where  $\hat{\eta}$ ,  $\hat{\eta}_{k1}$  and  $\hat{\eta}_{k2}$  ( $k = 1, 2$ ) can be obtained using Eqs. (B.16), (B.17) and (B.18).

$\hat{\mathbf{G}}_1^T \mathbf{Q}_1 (k = 1, 6, 7)$  can also be obtained using Eq. (56)

$$\hat{\mathbf{G}}_1^T \mathbf{Q}_k = -\frac{1}{l_c^2} \begin{bmatrix} \eta [0 & 1 & 0] \mathbf{N}_4 \mathbf{Q}_k \\ [0 & 1 & 0] \mathbf{N}_4 \mathbf{Q}_k \\ [0 & 0 & 1] \mathbf{N}_4 \mathbf{Q}_k \end{bmatrix} \bar{\mathbf{U}} + \begin{bmatrix} \mathbf{Q}_k^T \mathbf{A} \\ \mathbf{0}_{1 \times 12} \\ \mathbf{0}_{1 \times 12} \end{bmatrix}, \quad k = 1, 6, 7 \quad (\text{C.32})$$

Let

$$\mathbf{Q}_k = [\mathbf{Q}_k^{1T} \quad \mathbf{Q}_k^{2T} \quad \mathbf{Q}_k^{3T} \quad \mathbf{Q}_k^{4T}]^T, \quad k = 1,3,4,7,8. \quad (\text{C.33})$$

Then  $\hat{\mathbf{E}}_r \mathbf{Q}_1$  and  $\hat{\mathbf{E}}_r \mathbf{Q}_k (k = 1,3,4,7,8)$  can be obtained using Eq. (B.22)

$$\hat{\mathbf{E}}_r \mathbf{Q}_1 = -[\widetilde{\mathbf{Q}}_1^{1T} \quad \widetilde{\mathbf{Q}}_1^{2T} \quad \widetilde{\mathbf{Q}}_1^{3T} \quad \widetilde{\mathbf{Q}}_1^{4T}]^T \hat{\mathbf{w}}_r^e \quad (\text{C.34})$$

$$\hat{\mathbf{E}}_r \mathbf{Q}_k = \frac{\partial \dot{\mathbf{E}}_r}{\partial \dot{\mathbf{q}}} \mathbf{Q}_k = -[\widetilde{\mathbf{Q}}_1^{1T} \quad \widetilde{\mathbf{Q}}_1^{2T} \quad \widetilde{\mathbf{Q}}_1^{3T} \quad \widetilde{\mathbf{Q}}_1^{4T}]^T \mathbf{G}_1^T \mathbf{E}^T, \quad k = 1,3,4,7,8. \quad (\text{C.35})$$

## References

- [1] Tabarrok B, Leech CM, Kim YI. On the dynamics of an axially moving beam. J. Franklin Instit. 1974; 297(3): 201-220
- [2] Wang PKC, Wei JD. Vibrations in a moving flexible robot arm. J. Sound Vib. 1987; 116(1): 149-160
- [3] Mansfield L, Simmonds JG. The reverse spaghetti problem: drooping motion of an elastica issuing from a horizontal guide. ASME J. Appl. Mech. 1987; 54(1): 147-150
- [4] Stolte J, Benson RC. Dynamic deflection of paper emerging from a channel. ASME J. Vib. Acoust. 1992;114(2): 187-193
- [5] Behdinan K, Stylianou MC, Tabarrok B. Dynamics of flexible sliding beams - non-linear analysis part I: formulation. J. Sound Vib. 1997;208(4): 517-539
- [6] Behdinan K, Tabarrok B. Dynamics of flexible sliding beams - non-linear analysis

- part II: transient response. J. Sound Vib. 1997; 208(4): 541-565
- [7] McIver DB. Hamilton's principle for systems of changing mass. J. Eng. Math. 1973; 7(3): 249-261
- [8] Gürgöze M, Yüksel S. Transverse vibrations of a flexible beam sliding through a prismatic joint. J. Sound Vib. 1999; 223(3): 467-482
- [9] Stylianou M, Tabarrok B. Finite element analysis of an axially moving beam, part I: time integration. J. Sound Vib. 1994; 178(4): 433-453
- [10] Behdinan K, Tabarrok B. A finite element formulation for sliding beams. part I, Int. J. Numer. Methods Eng. 1998; 43(7): 1309-1333
- [11] Bathe KJ, Bolourchi S. Large displacement analysis of three-dimensional beam structures. Int. J. Numer. Methods Eng. 1979; 14(7): 961-986
- [12] Behdinan K, Stylianou MC, Tabarrok B. Co-rotational dynamic analysis of flexible beams. Comput. Methods Appl. Mech. Eng. 1998; 154(3-4): 151-161
- [13] Behdinan K, Stylianou MC, Tabarrok B. Sliding beams, part II: time integration. Int. J. Numer. Methods Eng. 1998; 43(7): 1335-1363
- [14] Humer A. Dynamic modeling of beams with non-material, deformation-dependent boundary conditions. J. Sound Vib. 2013; 332(3): 622-641
- [15] Steinbrecher I, Humer A, Vu-Quoc L. On the numerical modeling of sliding beams: a comparison of different approaches. J. Sound Vib. 2017; 408: 270-290
- [16] Dilpare AL. Transient nonlinear deflections of a cantilever beam of uniformly

- varying length by numerical methods. AIAA J. 1970; 8(12): 2293-2295
- [17] Banerjee AK, Kane TR. Extrusion of a beam from a rotating base. J. Guid. Control Dynam. 1989; 12(2): 140-146
- [18] Ashley H. Observations on the dynamic behavior of large flexible bodies in orbit. AIAA J. 1967; 5(3): 460-469
- [19] Canavin JR, Likins PW. Floating reference frames for flexible spacecraft. J. Spacecr. Rockets. 1977; 14(12): 724-732
- [20] Simo JC, Vu-Quoc L. On the dynamics of flexible beams under large overall motions - the plane case: part I. ASME J. Appl. Mech. 1986; 53(4): 849-854
- [21] Simo JC, Vu-Quoc L. On the dynamics of flexible beams under large overall motions - the plane case: part II. ASME J. Appl. Mech. 1986; 53(4): 855-863
- [22] Simo JC, Vu-Quoc L. On the dynamics in space of rods undergoing large motions - a geometrically exact approach. Comput. Methods Appl. Mech. Eng. 1988; 66(2), 125-161
- [23] Simo JC, Vu-Quoc L. Three-dimensional finite-strain rod model. Part II: Computational aspects. Comput. Methods Appl. Mech. Eng. 1986; 58(1), 79-116
- [24] Vu-Quoc L, Simo JC. On the dynamics of Earth-orbiting flexible satellites with multibody components. J. Guid. Control Dynam. 1987; 10(6), 549-558
- [25] Vu-Quoc, L. Dynamics of Flexible Structures Performing Large Overall Motions: A Geometrically-Nonlinear Approach. PhD thesis. University of California; 1986



- [26] McRobie FA, Lasenby J. Simo-Vu Quoc rods using Clifford algebra, *Int. J. Numer. Methods Eng.* 1999; 45(4), 377-398
- [27] Hestenes D, Sobczyk G. *Clifford Algebra to Geometric Calculus: A Unified Language for Mathematics and Physics*. Dordrecht: Reidel; 1984
- [28] Damaren C, Sharf I. Simulation of flexible-link manipulators with inertial and geometric nonlinearities. *ASME J. Dyn. Syst. Meas. Control.* 1995; 117(1): 74-87
- [29] Liu JY, Hong JZ. Geometric stiffening of flexible link system with large overall motion. *Comput. Struct.* 2003; 81(32): 2829-2841
- [30] Kane TR, Ryan RR, Banerjee AK. Dynamics of a cantilever beam attached to a moving base. *J. Guid. Control Dynam.* 1987; 10(2): 139-151
- [31] Yoo HH, Ryan RR, Scott RA. Dynamics of flexible beams undergoing overall motions. *J. Sound Vib.* 1995; 181(2): 261-278
- [32] Wu GY, He XS, Pai PF. Geometrically exact 3D beam element for arbitrary large rigid-elastic deformation analysis of aerospace structures. *Finite Elem. Anal. Des.* 2011; 47(4): 402-412
- [33] Yuh J, Young T. Dynamic modeling of an axially moving beam in rotation: simulation and experiment. *ASME J. Dyn. Syst. Meas. Control.* 1991; 113(1): 34-40
- [34] Vu-Quoc L, Li S. Dynamics of sliding geometrically-exact beams: large angle maneuver and parametric resonance. *Comput. Methods Appl. Mech. Eng.* 1995;

120(1-2): 65-118

- [35] Al-Bedoor BO, Khulief YA. Finite element dynamic modeling of a translating and rotating flexible link. *Comput. Methods Appl. Mech. Eng.* 1996; 131(1-2): 173-189
- [36] Kalyoncu M. Mathematical modelling and dynamic response of a multi-straight-line path tracing flexible robot manipulator with rotating-prismatic joint. *Appl. Math. Model.* 2008; 32(6): 1087-1098
- [37] Korayem MH, Shafei AM, Dehkordi SF. Systematic modeling of a chain of N-flexible link manipulators connected by revolute-prismatic joints using recursive Gibbs-Appell formulation. *Arch. Appl. Mech.* 2014; 84(2): 187-206
- [38] Korayem MH, Dehkordi SF. Derivation of dynamic equation of viscoelastic manipulator with revolute-prismatic joint using recursive Gibbs-Appell formulation. *Nonlinear Dyn.* 2017; 89(3): 2041-2064
- [39] Crisfield MA. A consistent co-rotational formulation for non-linear, three-dimensional, beam-elements. *Comput. Methods Appl. Mech. Eng.* 1990; 81(2): 131-150
- [40] Nour-Omid B, Rankin CC. Finite rotation analysis and consistent linearization using projectors. *Comput. Methods Appl. Mech. Eng.* 1991; 93(3): 353-384
- [41] Le TN, Battini JM, Hjiaj M. A consistent 3D corotational beam element for nonlinear dynamic analysis of flexible structures. *Comput. Methods Appl. Mech. Eng.* 2014; 269: 538-565

- [42] Reddy JN: On locking-free shear deformable beam finite elements. *Comput. Methods Appl. Mech. Eng.* 1997; 149(1-4): 113-132
- [43] Hilber HM, Hughes TJR, Taylor RL. Improved numerical dissipation for time integration algorithms in structural dynamics. *Earthq. Eng. Struct. D.* 1977; 5(3), 283-292
- [44] Crisfield MA. *Nonlinear Finite Element Analysis of Solids and Structures. Vol. 2, Advanced Topics.* Chichester: Wiley; 1997
- [45] Abraham R, Marsden JE, Ratiu T. *Manifolds, Tensor Analysis, and Applications.* New York: Springer; 2007
- [46] Behdinan K. Dynamics of geometrically nonlinear sliding beams. PhD thesis. University of Victoria; 1996
- [47] Battini JM, Pacoste C. Co-rotational beam elements with warping effects in instability problems. *Comput. Methods Appl. Mech. Eng.* 2002; 191(17-18): 1755-1789
- [48] Géradin M, Cardona A. *Flexible Multibody Dynamics: A Finite Element Approach.* Chichester : Wiley; 2001
- [49] Le TN, Battini JM, Hjjaj M. Dynamics of 3D beam elements in a corotational context: A comparative study of established and new formulations. *Finite Elem. Anal. Des.* 2012; 61: 97-111
- [50] Pacoste C. Co-rotational flat facet triangular elements for shell instability analyses.

- Comput. Methods Appl. Mech. Eng. 1998; 156(1-4): 75-110
- [51] Ibrahimbegovic A. On the choice of finite rotation parameters. Comput. Methods Appl. Mech. Eng. 1997; 149(1-4): 49-71
- [52] Le TN, Battini JM, Hjjaj M. Efficient formulation for dynamics of corotational 2D beams. Comput. Mech. 2011; 48(2): 153-161
- [53] Hsiao KM, Lin JY, Lin WY. A consistent co-rotational finite element formulation for geometrically nonlinear dynamics analysis of 3-D beams. Comput. Methods Appl. Mech. Eng. 1999; 169(1/2): 1-18